www.impactjournals.com/oncotarget/ Oncotarget, 2018, Vol. 9, (No. 17), pp: 13593-13611

Research Paper

Adenosine A_{2A} receptor ligand recognition and signaling is blocked by A_{2B} receptors

Sonja Hinz[1], Gemma Navarro[2,4], Dasiel Borroto-Escuela[3], Benjamin F. Seibt[1], York-Christoph Ammon[1], Elisabetta de Filippo[1], Azeem Danish[1], Svenja K. Lacher[1], Barbora Červinková[1], Muhammad Rafehi[1], Kjell Fuxe[3], Anke C. Schiedel[1], Rafael Franco[2,4] and Christa E. Müller[1]

[1]PharmaCenter Bonn, Pharmaceutical Institute, Pharmaceutical Chemistry I, University of Bonn, Bonn, Germany

[2]Department of Biochemistry and Molecular Biomedicine, Faculty of Biology, University of Barcelona, Barcelona, Spain

[3]Department of Neuroscience, Karolinska Institutet, Stockholm, Sweden

[4]Centro de Investigación en Red, Enfermedades Neurodegenerativas (CIBERNED), Instituto de Salud Carlos III, Madrid, Spain

Correspondence to: *Christa E. Müller,* ***email:*** *christa.mueller@uni-bonn.de*

Keywords: *adenosine receptors (ARs); G protein-coupled receptor (GPCR); immuno-oncology; pharmacology; receptor heteromerization*

Received: *November 08, 2017* ***Accepted:*** *January 30, 2018* ***Published:*** *February 06, 2018*

ABSTRACT

The adenosine receptor (AR) subtypes A_{2A} and A_{2B} are rhodopsin-like G_s protein-coupled receptors whose expression is highly regulated under pathological, e.g. hypoxic, ischemic and inflammatory conditions. Both receptors play important roles in inflammatory and neurodegenerative diseases, are blocked by caffeine, and have now become major drug targets in immuno-oncology. By Förster resonance energy transfer (FRET), bioluminescence resonance energy transfer (BRET), bimolecular fluorescence complementation (BiFC) and proximity ligation assays (PLA) we demonstrated A_{2A}-A_{2B}AR heteromeric complex formation. Moreover we observed a dramatically altered pharmacology of the A_{2A}AR when co-expressed with the A_{2B}AR ($A_{2B} \geq A_{2A}$) in recombinant as well as in native cells. In the presence of A_{2B}ARs, A_{2A}-selective ligands lost high affinity binding to A_{2A}ARs and displayed strongly reduced potency in cAMP accumulation and dynamic mass redistribution (DMR) assays. These results have major implications for the use of A_{2A}AR ligands as drugs as they will fail to modulate the receptor in an A_{2A}-A_{2B} heteromer context. Accordingly, A_{2A}-A_{2B}AR heteromers represent novel pharmacological targets.

INTRODUCTION

Adenosine receptors (ARs) are G protein-coupled receptors (GPCRs) activated by the nucleoside adenosine. Four subtypes designated A_1, A_{2A}, A_{2B} and A_3ARs exist. A_1 and A_3ARs preferentially couple to $G_{i/o}$ proteins mediating inhibition of adenylate cyclase (AC) activity, while A_{2A} and A_{2B} receptors couple to $G_{s/olf}$ proteins leading to AC activation and subsequent increase in cAMP formation [1]. In addition, A_{2B} and A_3ARs were shown to couple to G_q proteins which results in phospholipase C activation followed by a rise in inositol trisphosphate levels mediating intracellular calcium release [2–3]. The A_{2A}AR is expressed in high density in the caudate-putamen, and at low levels in most other brain regions. In the periphery, the A_{2A}AR is highly expressed in cells of the immune system and blood platelets, and at lower levels in many other cells and organs [4]. The A_{2B}AR is broadly expressed but mostly at moderate to low levels. A_{2A} and A_{2B}ARs are the most closely related AR subtypes with an overall sequence identity of 58% and a similarity of 73% [5]. They are co-expressed on many different cell types and in various organs and tissues, e.g. in heart [6], myeloid cells [7], T-cells [8], blood platelets [9], brown and white adipocytes [10], and in many tumors, e.g. neuroendocrine tumors [11], ovarian cancer [12], and prostate cancer

[13]. The expression of A_{2A} and A_{2B}ARs and their relative proportion can be markedly altered under pathological conditions [14]. For example, increased A_{2A}AR expression is observed in the brains of patients suffering from neurodegenerative diseases [15], in multiple sclerosis and in amyotrophic lateral sclerosis [16–17]. Upon activation of T-lymphocytes the A_{2A}AR is considerably upregulated [18]. On the other hand, the expression of A_{2B}ARs can be drastically increased in a hypoxia-inducible factor-(HIF1α-) dependent manner under hypoxic conditions, e.g. in inflamed or ischemic tissue, in tumors and cancer cells [19–20]. Hypoxia induction leads to a decrease in A_{2A}AR expression while increasing A_{2B}AR expression in human umbilical vein endothelial and bronchial smooth muscle cells. Pharmacological responses of A_{2A}/A_{2B}AR agonists were significantly altered in these cells [21]. The well investigated A_{2A}AR subtype, the so-called "high-affinity A_2AR receptor", is typically activated by relatively low (nanomolar) concentrations of adenosine, mediating potent anti-inflammatory and immunosuppressant as well as hypotensive and anti-psychotic effects [22]. In contrast, activation of the A_{2B}AR subtype, the "low-affinity A_2AR", requires high, micromolar adenosine concentrations for activation [4]. Extracellular adenosine levels can rise from basal values of around 100 nM by up to 100-fold reaching concentrations of around 10 μM under pathological, i.e. hypoxic, ischemic or inflammatory conditions [1, 4, 23]. Cell death can lead to the formation of large amounts of extracellular adenosine through enzymatic degradation of released ATP by ectonucleotidases (CD39, CD73), e.g. in solid tumors [24]. Both anti- as well as pro-inflammatory effects have been associated with the A_{2B}AR [25], and the reasons for these contradictory results have remained obscure. The physiological significance of the A_{2B}AR subtype is scarcely understood so far. During the last decade it has become well accepted that GPCRs are able to form di- or oligomeric assemblies of identical or distinct receptor monomers [26]. Most of these complexes have been detected in transfected living cells using well accepted biophysical techniques such as resonance energy transfer (bioluminescence and Förster resonance energy transfer, BRET and FRET) or bimolecular fluorescence complementation (BiFC) assays [27–28]. Proximity ligation assays (PLA) have been developed for identifying receptor heteromers in native cells and tissues [29]. Heteromer formation may modulate receptor pharmacology such as the affinity and potency of ligands or G protein coupling and signaling [30–31]. Recently, structural models of GPCR oligomers associated with G proteins have been built [32], and the development of heteromer-selective receptor ligands is becoming a promising new research area [33]. The A_{2A}AR was reported to form homomeric receptor complexes as well as heteromers with several other GPCRs including dopamine D_2 and D_3, cannabinoid CB_1, nucleotide $P2Y_1$ and $P2Y_2$, and A_1ARs [1]. Especially A_{2A}-D_2 heteromeric receptor complexes have been intensively studied since they play a significant role in Parkinson's disease [34]. However, homo- or heteromer formation of the A_{2B}AR subtype has not been demonstrated up to now. Based on the frequent co-expression of the closely related AR subtypes A_{2A} and A_{2B}, and considering the up-regulation of the A_{2B}AR subtype and the up- or down-regulation of the A_{2A}AR under many pathological conditions, the question arises if both receptors could form heteromers and whether this might affect their pharmacology and signaling. Here we demonstrate that A_{2A}-A_{2B}AR heteromers are formed in living cells by employing FRET, BRET and PLA, and their presence in native tissue was confirmed. Heteromer formation was found to be independent of the presence of agonists or antagonists, and does not require the long C-terminus of the A_{2A}AR. Importantly, we demonstrate that A_{2A}-A_{2B} heteromerization is the reason for drastically altered pharmacology, in particular for the A_{2A}AR, which is completely blocked by the presence of A_{2B}AR protein. These results can now help to explain many unexpected or previously misinterpreted observations. They will be of high relevance for recently started drug development programs targeting A_{2A} or A_{2B}ARs, in particular in neurodegenerative diseases and immuno-oncology.

RESULTS

FRET, BRET and BiFC experiments

FRET is a powerful technique for measuring protein-protein interactions in living cells [35]. To investigate a possible A_{2A}-A_{2B}AR interaction, FRET experiments were performed in Chinese hamster ovary (CHO-K1) cells transiently transfected with fusion proteins of green fluorescent protein variant 2 (GFP^2) and enhanced yellow fluorescent protein (EYFP) attached to the C-terminus of the receptors [36] (Figure 1A–1C). The previously described A_{2A}-homodimer and the fusion protein GFP^2-EYFP were employed as positive controls showing FRET efficiencies of 0.23 and 0.44, respectively, similar to those previously reported (A_{2A} homodimer: 0.28, GFP^2-EYFP: 0.52) (Figure 1A, 1B) [37]. The fusion protein GFP^2-EYFP displayed a high FRET efficiency due to the very close proximity of donor and acceptor as a result of the short linker between both fluorophores. A clear FRET signal with an efficiency of 0.16 was observed in the co-transfected cells indicating the formation of A_{2A}-A_{2B} heteroreceptor complexes (Figure 1A). The pair A_{2A}AR and $GABA_{B2}$ receptor [36–37] was employed as a negative control; it showed a very low FRET signal demonstrating the specificity of the observed interactions (Figure 1A–1B). To gain insight into the potential A_{2A}-A_{2B} heteromer interface, the C-terminal tail of the A_{2A}AR was removed and the resulting construct A_{2A}1-293R-EYFP was studied in FRET experiments as an acceptor fluorophore in combination with the A_{2B}-GFP^2 donor

fluorophore. The results indicated that the A_{2A}AR that was lacking the C-terminal domain was still fully able to form heteromers with the A_{2B}AR (FRET efficiency 0.24, Figure 1B) suggesting that different receptor domains, possibly helical domains, have to be involved in heteromer formation.

BRET is another biophysical technique that can be utilized to detect protein-protein interactions by measuring energy transfer from a bioluminescence donor to a fluorescent acceptor [35]. To confirm a direct A_{2A}-A_{2B}AR interaction, BRET experiments were performed in living CHO-K1 cells transiently expressing fusion proteins

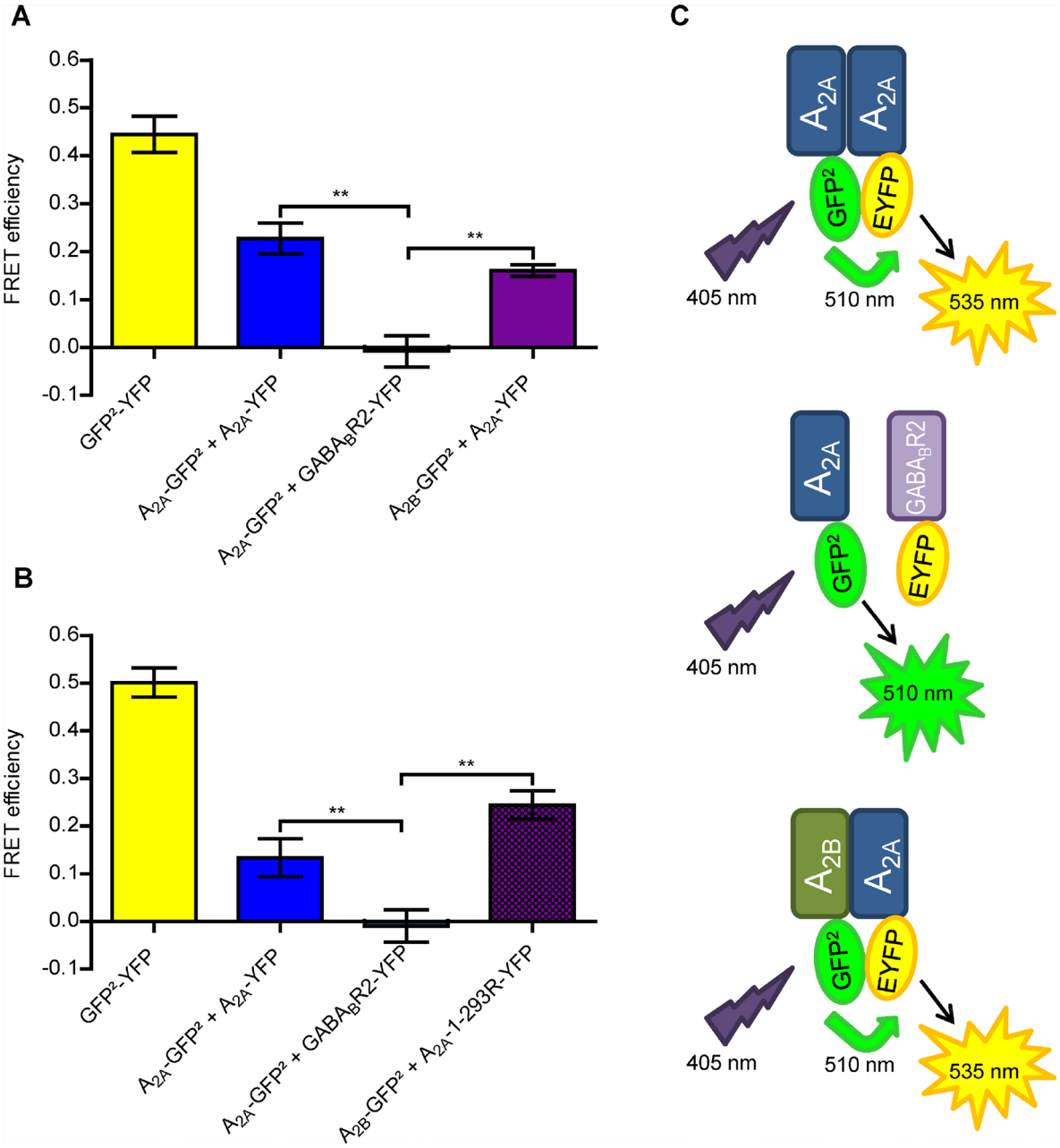

Figure 1: Biophysical assays using A_{2A} and A_{2B}ARs fused to FRET donor and acceptor. (**A**) FRET efficiencies were calculated by a sensitized emission method in living CHO cells transiently transfected with the different plasmids. Data are means ± SEM of 4–5 independent experiments performed in duplicates. The one-way ANOVA with Dunnett's post-hoc test showed significant differences in A_{2A}-GFP² + A_{2A}-EYFP (positive control) or A_{2B}-GFP² + A_{2A}-EYFP versus the negative control (A_{2A}-GFP² + $GABA_BR2$-EYFP), $^{**}p < 0.01$. As an internal control the fusion protein GFP²-EYFP was used. (**B**) FRET efficiencies determined in CHO cells transiently transfected with the different plasmids. The same controls were used as shown in (**A**). Data are means ± SEM of 5 independent experiments performed in duplicates. The one-way ANOVA with Dunnett's post-hoc test showed significant differences between A_{2A}-GFP² + A_{2A}-EYFP (positive control) or A_{2B}-GFP² + A_{2A}-1-293-EYFP versus the negative control (A_{2A}-GFP² + $GABA_BR2$-EYFP), $^{**}p < 0.01$. (**C**) Schematic representation of the performed FRET experiments with the different donor/acceptor pairs.

consisting of a receptor (A_{2A}, A_{2B}, D_2, or $GABA_{B2}$) and Rluc (*Renilla luciferase*) or the fluorescent protein EYFP attached to the C-terminus (Figure 2A–2D). Three kinds of experiments were performed as shown in Figure 2A, 2C and 2D. For BRET saturation curves cells were co-transfected with a constant amount of cDNA for Rluc-receptor constructs and increasing concentrations of cDNAs for EYFP-receptor constructs. As a widely accepted positive control for GPCR dimers, donor/aceptor proteins having the dopamine D_2R-A_{2A}AR were used. The results showed a high BRET signal displaying a hyperbolic curve, with a $BRET_{50}$ value of 239 ± 40 and a $BRET_{max}$ value of 144 ± 6 mBU. As a negative control, donor/acceptor proteins having the A_{2A}AR and $GABA_{B2}$ receptor pair were used. The combination of A_{2A} and A_{2B}ARs resulted in a specific BRET signal which was even higher than the positive control indicating a specific interaction of both receptors. A $BRET_{50}$ value of 122 ± 6 and a $BRET_{max}$ value of 158 ± 10 mBU were determined (Figure 2A). Subsequently, a BRET displacement study was performed in which increasing amounts of unlabeled A_{2B}AR were added to A_{2B}-Rluc and A_{2A}-YFP receptors. The experiment showed a significant decrease in the BRET signal, which was dependent on the added amount of unlabeled A_{2B}AR (Figure 2C), indicating displacement by the unlabeled receptor of the Rluc-tagged A_{2B}AR in the heteromer. As a final step, potential effects of A_{2A} and A_{2B}AR agonists and antagonists on A_{2A}-A_{2B} heteromer formation were studied. The BRET signal after 60 min of treatment with agonists (adenosine, nonselective; NECA, nonselective; CGS-21680, A_{2A}-selective; BAY60–6583, A_{2B}-selective) or

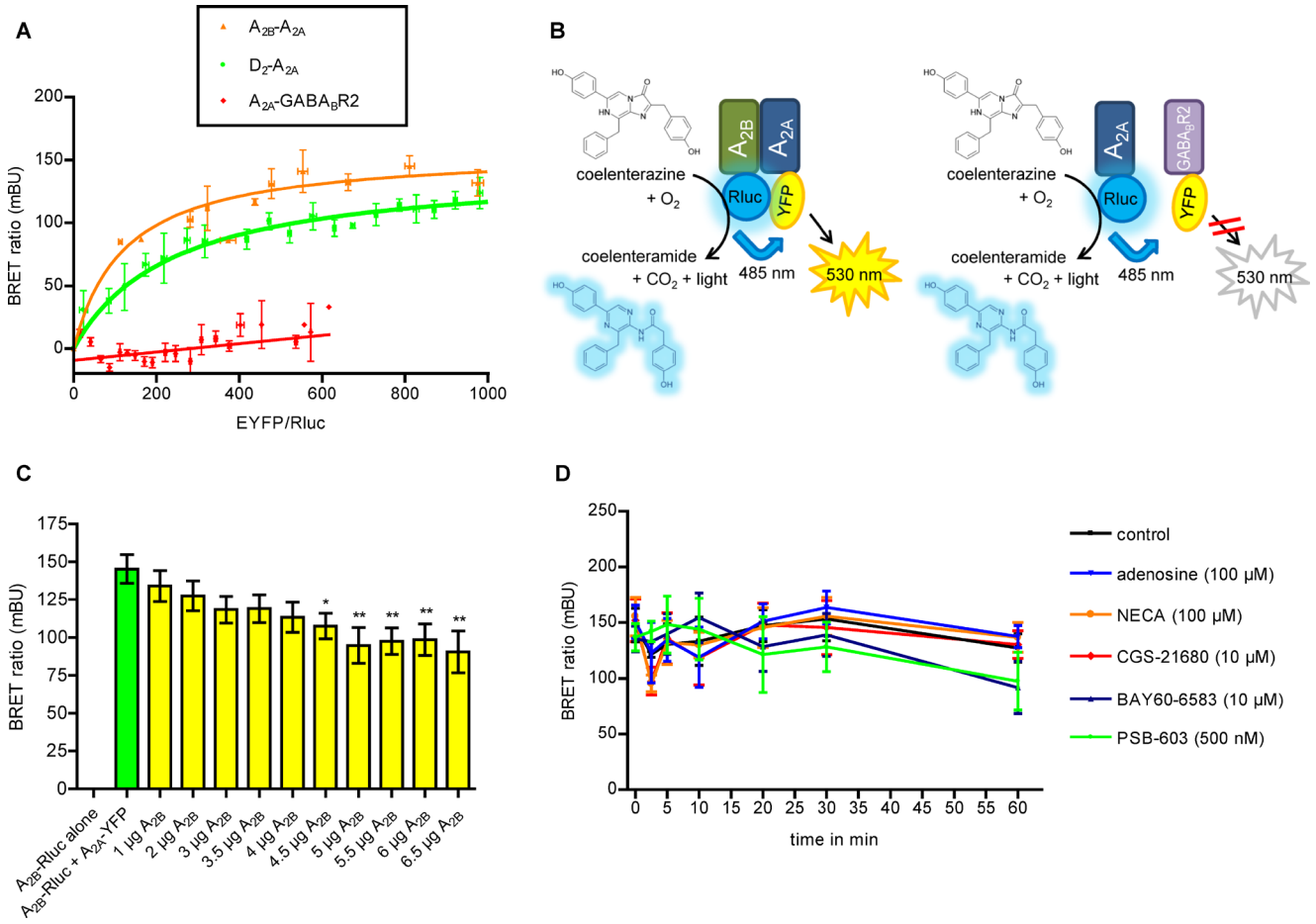

Figure 2: Biophysical assays using A_{2A} and A_{2B}ARs fused to BRET donor and acceptor. (**A**) BRET saturation curves: CHO-K1 cells were transiently co-transfected with a constant amount of A_{2A}, A_{2B} or D_2 receptors fused to *Rluc* and increasing amounts of cDNA for A_{2A} or $GABA_{B2}$ receptors fused to EYFP. BRET experiments were performed in duplicates for A_{2B}-Rluc and A_{2A}-YFP (▲) (n =11) with a $BRET_{max}$ = 158 ± 10 mBU and $BRET_{50}$ = 122 ± 58, positive control D_2-Rluc and A_{2A}-YFP (●) (n = 15) $BRET_{max}$ = 144 ± 6 mBU and $BRET_{50}$ = 239 ± 40, and negative control A_{2A}-Rluc and $GABA_{B2}$-YFP (♦) (n = 13). (**B**) Schematic representation of the BRET experiments. (**C**) BRET competition experiments were performed (n = 4, in triplicates) in cells transfected with 1.25 µg of cDNA for A_{2B}-Rluc, 2.5 µg of cDNA for A_{2A}-YFP and increasing amounts of cDNA for untagged A_{2B}ARs. The one-way ANOVA with Dunnett's post-hoc test showed a significant decrease in the BRET signal compared to cells which were not transfected with untagged A_{2B}ARs (green column; $^{*}p < 0.05$; $^{**}p < 0.01$). (**D**) CHO cells were transiently co-transfected with 2 µg of cDNA for A_{2B}-Rluc and 3 µg of cDNA for A_{2A}-YFP. Different agonists (adenosine, NECA, CGS-21680, BAY60-6583) and antagonists (PSB-603) were added and the BRET signal was measured over a time period of 60 min (n = 3, in duplicates).

the A_{2B} antagonist PSB-603 was similar to that obtained in the absence of ligands (Figure 2D), thus indicating that A_{2A}-A_{2B} heteromer formation was not influenced by those receptor ligands.

These results were further corroborated by BiFC experiments, which provided strong evidence for a very close interaction between A_{2A} and A_{2B}ARs (Supplementary Figures 1, 2).

In situ proximity ligation experiments in the rat brain

The PLA combines the high specificity and affinity of antibodies (PLA probe) with the sensitivity of quantitative polymerase chain reactions (PCR) to detect proteins that are forming molecular complexes in native sources [38]. Initially we studied the recombinant CHO-A_{2A}-A_{2B} cell line to investigate the receptors' proximity (Supplementary Figure 3A–3C) and obtained small, brightly green fluorescent spots each of which represents a single A_{2A}-A_{2B}AR heteromer (Supplementary Figure 3C). Next we performed *in situ* PLA focusing on the dorsal hippocampus of the rat brain (Figure 3, Supplementary Figures 4, 5) where moderate to high densities of PLA-specific clusters were found. It should be noted that the molecular layer of the dentate gyrus lacked PLA clusters, and the unspecific labeling there was similar to that observed in negative control sections obtained by omitting the primary anti-A_{2A} antibody. Furthermore, few PLA positive clusters were observed in the oriens of the *CA1* areas. In contrast, a high density of A_{2A}-A_{2B} specific clusters was found in the *CA3* pyramidal cell layer, mainly in perisomatic location (Figure 3), where PLA-positive clusters had diameters from 0.5–2 µm. They were present also in lower densities in the radiatum and oriens. In all these regions PLA positive clusters were also found in the neuropil. The *CA1* showed a similar distribution pattern (as compared with *CA3*), with high dot/cluster densities within the pyramidal cell layer. An important difference was, however, the diameter range of the clusters, which appeared to be reduced in this *CA1* region versus *CA3* (Supplementary Figure 4).

In the polymorphic layer of the dentate gyrus (PoDG), a high density of specific A_{2A}-A_{2B} clusters was observed in both perisomatic and neuropil position. The range of diameter size in the clusters was similar to that in the *CA3* area (Supplementary Figure 5).

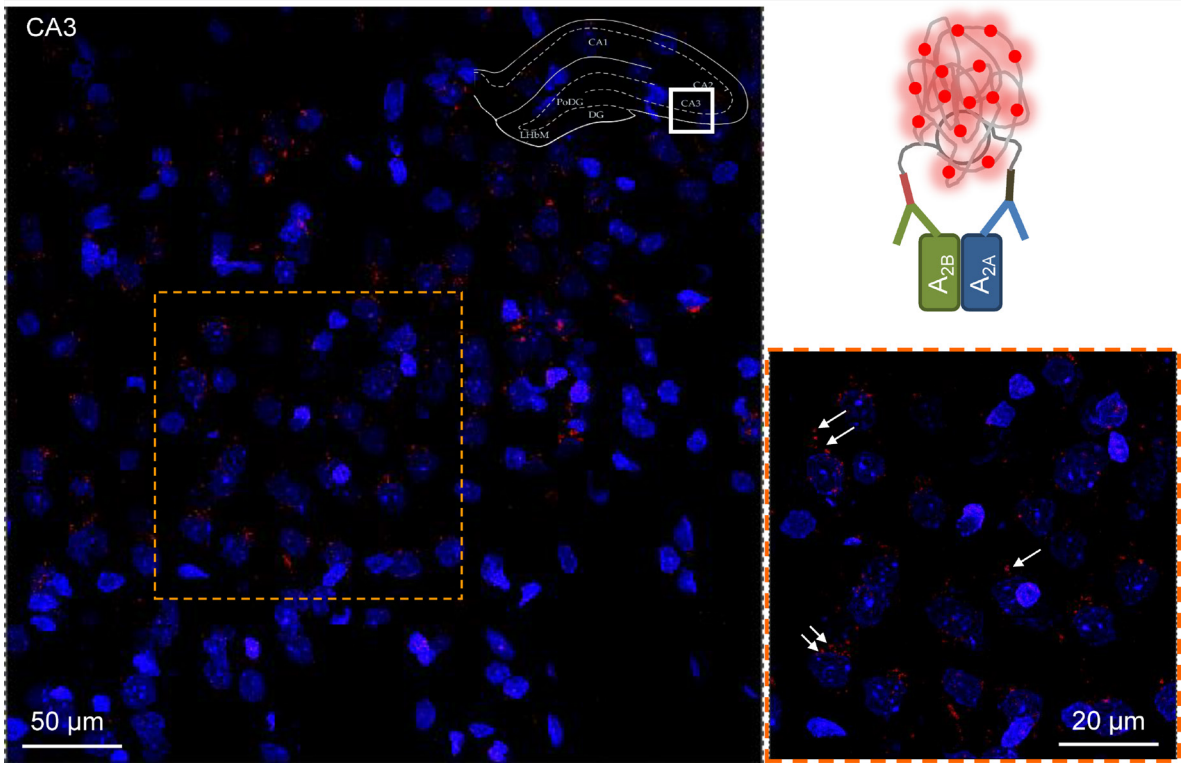

Figure 3: *In situ* proximity ligation assay in rat hippocampus. A_{2A}-A_{2B}AR-specific PLA clusters in the *CA3* region of the *dorsal hippocampus* of the rat (Bregma: –3.6 mm). The sampled region is taken from the framed section of the dorsal hippocampus in the upper right corner of the figure. The microphotographs taken are based on 20 Z-scans (1 µm each). The nuclei are shown in blue. A high density of PLA positive clusters in red are visualized mainly in the pyramidal cell layer shown also in higher amplification in the panel at the lower right part of the figure. A few are indicated by arrows. The diameter range of the clusters is 0.5–2 µm. They are mainly located in a perisomatic position around the blue nuclei but also in the neuropil. A low density of specific PLA clusters is also found in the radiatum and oriens close to the pyramidal cell layer.

Pharmacological implications of A_{2A}-A_{2B}AR heteromer formation

To study the pharmacology of A_{2A}-A_{2B}AR heteromers, native as well as recombinant cell lines were investigated. Expression levels of A_{2A} and A_{2B}ARs were analyzed by reverse transcriptase (RT) PCR, Western blot analysis and radioligand binding studies (Supplementary Figure 6A–6E). Recombinant cell lines were prepared to control the proportion of A_{2A} and A_{2B}AR expression ($A_{2B} \geq A_{2A}$, and $A_{2A} > A_{2B}$) (Supplementary Table 1).

Radioligand-receptor binding studies

Radioligand binding studies were performed using the A_{2B}-selective antagonist radioligand [^{3}H] PSB-603 and two A_{2A}-selective radioligands, the antagonist [^{3}H]MSX-2, and the agonist [^{3}H]CGS-21680 (Supplementary Figure 7A–7C, Supplementary Table 2). A selective radiolabeled agonist for A_{2B}ARs is currently not available. Labeling of A_{2B}ARs with [^{3}H]PSB-603 demonstrated high A_{2B} expression in membrane preparations of CHO-A_{2B} and CHO-A_{2A}-A_{2B} ($A_{2B} \geq A_{2A}$) cell lines both of which displayed similar A_{2B} expression levels (502 and 418 fmol/mg protein, respectively). Jurkat-T (220 fmol/mg protein) and HeLa cells (80 fmol/mg protein) had lower A_{2B}AR expression levels (Supplementary Figure 6E, Supplementary Table 2). As expected, in cells lacking significant A_{2B} expression (CHO-K1, CHO-HA-A_{2A}, HEK-A_{2A}), no high-affinity binding of the A_{2B}-selective antagonist radioligand [^{3}H]PSB-603 was observed (Supplementary Figure 7C). In cells that co-expressed both receptors (CHO-A_{2A}-A_{2B} cells, HeLa cells, Jurkat-T cells, native human T-lymphocytes), specific binding of [^{3}H]PSB-603 was detected, and its affinity was similar to that determined at CHO cells expressing only A_{2B}ARs (Supplementary Figure 8A, Supplementary Table 2). Native primary human lymphocytes displayed a moderate expression level of A_{2B}ARs, lower to that of A_{2A}ARs. Upon activation with phytohemagglutinin (PHA), the A_{2B} expression level remained virtually unaltered (Supplementary Figure 9). All radioligand binding results on A_{2B}ARs were in agreement with the data obtained in RT-PCR and Western blot experiments (Supplementary Figure 6A–6D, Supplementary Table 2). The A_{2A}-selective radioligands [^{3}H]MSX-2 and [^{3}H] CGS-21680 labeled A_{2A}ARs in CHO-A_{2A} cells and in cells expressing more A_{2A}- than A_{2B}ARs (Figure 4, Supplementary Figure 7A, 7B, Supplementary Table 2). Native primary human lymphocytes displayed specific binding of [^{3}H]MSX-2 indicating A_{2A}AR expression, that was significantly upregulated (by about 4-fold) upon activation with PHA (Supplementary Figure 9, Supplementary Table 2). Unexpectedly, in cells with similar or higher expression of A_{2B} as compared to A_{2A}ARs no high-affinity binding of either A_{2A}-selective radioligand, [^{3}H]MSX-2 or [^{3}H]CGS-21680, was observed (Supplementary Figure 8A, 8B, Supplementary Table 2). Competition binding assays versus [^{3}H]PSB-603 were performed to determine the A_{2B} affinity of selected agonists and antagonists while A_{2A} affinity of compounds was determined versus [^{3}H]MSX-2. Indeed, the latter was only possible in cell lines expressing more A_{2A} than A_{2B}ARs since high affinity binding of the A_{2A}-selective radioligands was abolished when A_{2B} receptors were co-expressed (see above).

CHO-A_{2A} and CHO-A_{2B} cell lines displayed the expected affinities of agonists and antagonists typical for, respectively, A_{2A} or A_{2B}ARs (Figure 4A, 4B, Supplementary Table 3). In CHO-A_{2A}-A_{2B} cell membranes, which showed a similar or slightly higher expression of A_{2B} than of A_{2A}ARs, the agonists adenosine, NECA, and BAY60-6583 and the antagonists PSB-603 and caffeine displayed only slightly modulated A_{2B} affinities (Figure 4A, 4B, Supplementary Table 3). We subsequently studied a T-cell line, namely Jurkat-T cells, which express similar amounts of A_{2A} and A_{2B}ARs, the level of which is, however, lower than in the recombinant CHO-A_{2A}-A_{2B} cells. The A_{2B}-selective radioligand [^{3}H]PSB-603 displayed high affinity binding which was displaced by the A_{2B}-selective partial agonist BAY60-6583 (Figure 4C, Supplementary Figure 8A, Supplementary Tables 2, 3). However, no high-affinity binding was observed for the A_{2A}-selective radioligands [^{3}H]MSX-2 and [^{3}H]CGS-21680 (Supplementary Figure 8A, 8B, Supplementary Table 2), although we could clearly detect A_{2A}AR protein expression in Jurkat-T cells (Supplementary Figure 6C). In native T-lymphocytes, isolated from healthy human blood donors, the expression of the A_{2A}AR was higher than that of the A_{2B}AR (Supplementary Figure 9, Supplementary Table 2). High affinity binding was then observed for the A_{2A}-selective radioligand [^{3}H]MSX-2 as well as for the A_{2B}-selective radioligand [^{3}H]PSB-603 (Supplementary Figure 8A, 8B, Supplementary Table 2). In HeLa cells, which natively express more A_{2B} than A_{2A}ARs, again, no high-affinity binding was obtained for the A_{2A}-selective radioligands [^{3}H]MSX-2 and [^{3}H]CGS-21680 (Supplementary Figure 8A, 8B, Supplementary Table 2) although we could clearly detect the A_{2A}AR protein in this cell line (Supplementary Figure 6D). As a next step we overexpressed the human A_{2A}AR containing an HA tag in HeLa cells to obtain a cell line which expressed more A_{2A} than A_{2B}ARs (Supplementary Figure 6D, Supplementary Table 2). This led to the recovery of high-affinity binding for the A_{2A}-selective radioligands (Figure 4D, Supplementary Table 2). NECA and CGS-21680 showed higher affinity versus the agonist radioligand than versus the antagonist radioligand, whereas the antagonist MSX-2 displayed similar affinities versus both radioligands (Figure 4D, Supplementary Table 3), results that are typical for A_{2A}ARs [39].

cAMP accumulation assays

A_{2A} and A_{2B}ARs are coupled to G_s proteins, activating adenylate cyclase. Thus, cAMP accumulation assays were performed at CHO cells stably expressing the A_{2A}AR, the A_{2B}AR, or both. Adenosine increased cAMP accumulation with an EC_{50} value of 174 nM in CHO cells expressing the "high affinity" A_{2A}AR, and with an EC_{50} value of 12,500 nM in CHO cells expressing the "low-affinity" A_{2B}AR. The CHO-A_{2A}-A_{2B} cell line co-expressing both subtypes showed virtually the same EC_{50} value (13,100 nM) as the cell line *only* expressing A_{2B}ARs (Figure 5A, Supplementary Table 4). The metabolically more stable adenosine analog NECA displayed a similar behaviour. The potent A_{2A}-selective agonist CGS-21680 (EC_{50} 16.6 nM in CHO-A_{2A} cells) was inactive in CHO-A_{2A}-A_{2B} cells (EC_{50} > 10,000 nM). In contrast, the A_{2B}-selective partial agonist BAY60-6583 (EC_{50} 165 nM in A_{2B}AR-expressing cells) had similar potency in the A_{2A}-A_{2B}-coexpressing cell line (EC_{50} 193 nM) (Figure 5A, Supplementary Table 4). Antagonist potencies were determined by measuring concentration-response curves for the non-selective agonist NECA in the presence or absence of different antagonists, and K_B values were calculated. The A_{2B}-selective antagonist PSB-603 and the non-selective antagonist caffeine showed very similar K_B-values at CHO-A_{2A}-hA_{2B} (PSB-603, K_B 0.673 nM; caffeine, K_B 9,900 nM) as at CHO-A_{2B} cells (PSB-603, K_B 0.358 nM; caffeine, K_B 15,600 nM) (Figure 5B, Supplementary Table 4).

We next employed Jurkat-T cells as a native cell line expressing similar amounts of A_{2A} and A_{2B}ARs. These cells behaved like the CHO-A_{2A}-A_{2B} cell line displaying moderate potency for the physiological agonist adenosine and the structurally related agonist NECA. Again, CGS-21680 was inactive at concentrations up to 10 µM, while the A_{2B}-selective antagonist PSB-603 and the nonselective antagonist caffeine displayed K_B-values in the same

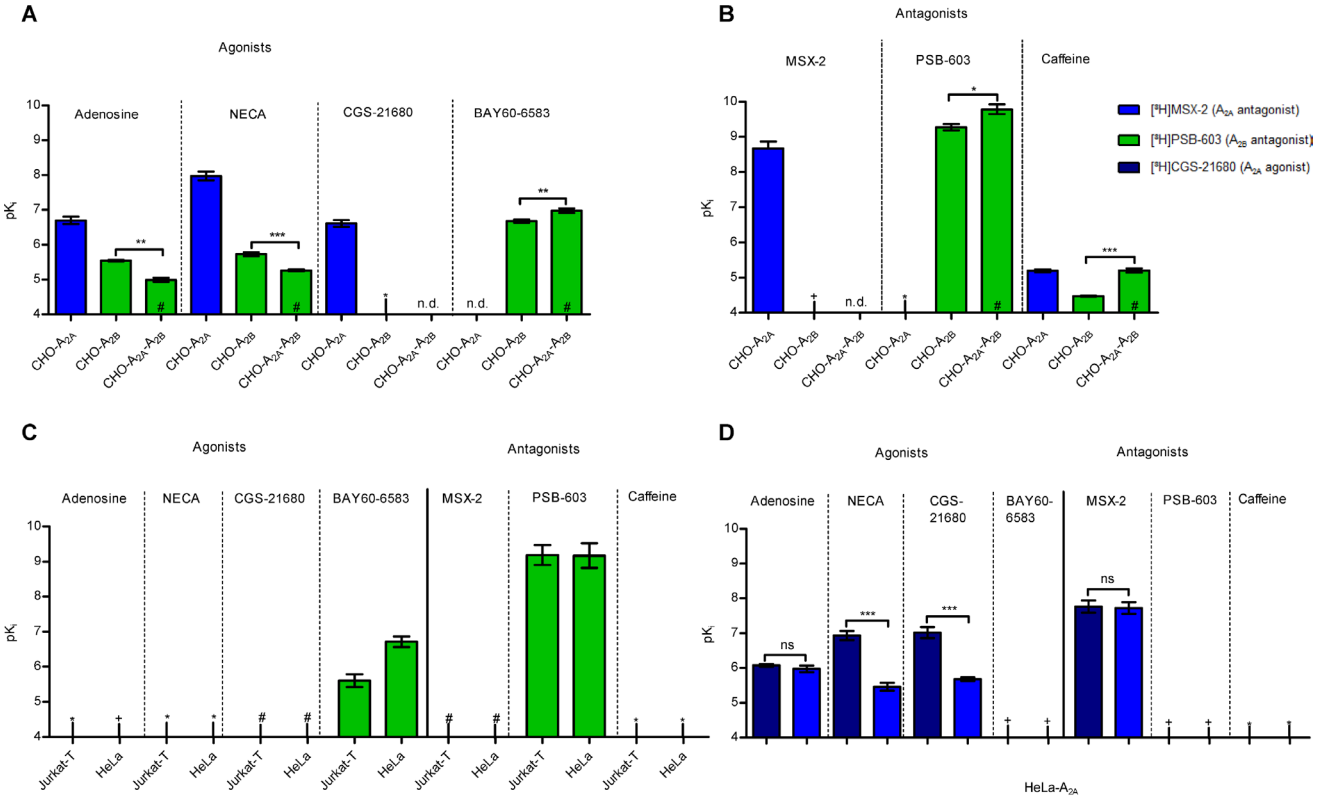

*tested, pKi < 5; +tested, pKi < 6; #No high affinity binding for [³H]CGS-21680 and [³H]MSX-2 was detectable at CHO-A_{2A}-A_{2B}, Jurkat-T and HeLa membranes; n.d. not determined

Figure 4: Affinities of AR agonists and antagonists in different cells expressing A_{2A} and A_{2B}ARs. (**A**) Competition binding experiments of agonists versus 1 nM [³H]MSX-2 at A_{2A}-expressing membranes, and versus 0.3 nM [³H]PSB-603 at A_{2B}- and at A_{2A}-A_{2B}AR-expressing membranes of CHO cells. The two-tailed *t*-test showed significant differences. $^{***}p < 0.001$, $^{**}p < 0.01$, n = 2–3, see also Supplementary Table 3. (**B**) Competition binding experiments of AR antagonists versus 1 nM [³H]MSX-2 at A_{2A}-expressing, and versus 0.3 nM [³H]PSB-603 at A_{2B} - and at A_{2A}-A_{2B}AR co-expressing CHO cell membranes. The two-tailed *t*-test showed significant differences. $^{***}p < 0.001$, $^{*}p < 0.1$, n = 3, see also Supplementary Table 3. (**C**) Competition binding experiments of AR agonists and antagonists versus 0.3 nM [³H]PSB-603 at Jurkat-T and HeLa cell membranes, n = 3–6, see also Supplementary Table 3. (**D**) Competition binding experiments agonists and antagonists versus 5 nM [³H]CGS-21680, and versus 1 nM [³H]MSX2, respectively, at HeLa cell membranes recombinantly overexpressing A_{2A}ARs. The two-tailed *t*-test showed significant differences. ns: not significant, $^{***}p < 0.001$, n = 3–4, see also Supplementary Table 3.

range as those determined at CHO-A_{2B} cells (Figure 5C, Supplementary Table 4).

cAMP assays at HEK-A_{2A} cells transiently transfected with increasing amounts of A_{2B}AR

Next, the effect of the expression of different amounts of A_{2B}ARs on A_{2A}AR pharmacology was studied. To this end human embryonic kidney (HEK293T) cells stably expressing the human A_{2A}AR were transfected with human A_{2B}AR cDNA to transiently express increasing amounts of A_{2B}ARs. The A_{2B}-selective agonist BAY60-6583 (100 nM) showed a significant increase in cAMP accumulation with increasing amounts of transiently transfected A_{2B}ARs confirming functionality of the A_{2B}AR (Figure 6A). In contrast, when stimulating the cells with the A_{2A}-selective agonist CGS-21680 (100 nM), a significant decrease in cAMP accumulation with increasing amounts of the transiently transfected A_{2B}AR was observed suggesting an inhibition of the A_{2A}AR

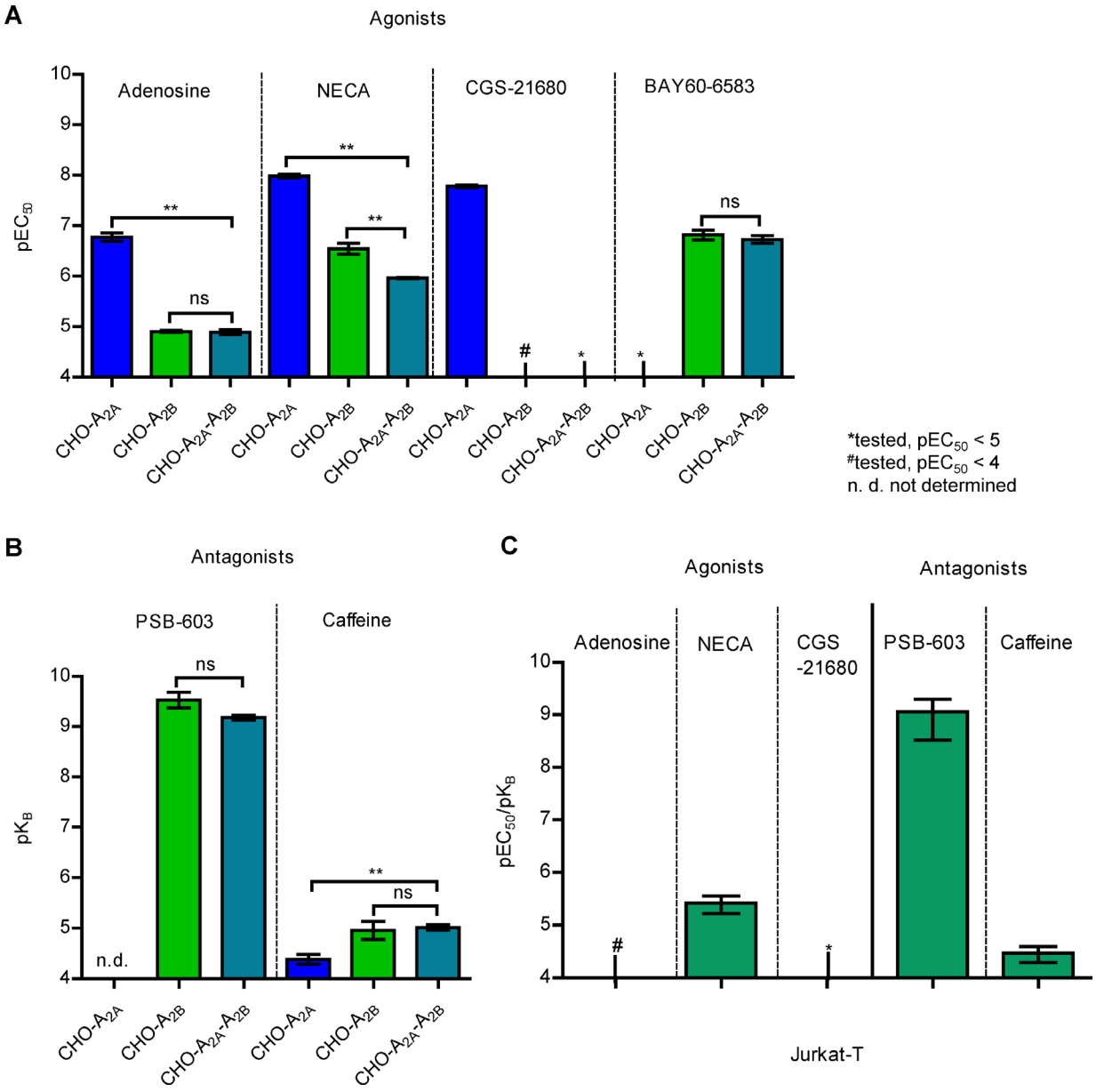

Figure 5: cAMP accumulation in recombinant CHO cell lines and in Jurkat-T cells. (**A**) pEC_{50} values of AR agonists in cAMP accumulation assays in CHO-$A_{2A,}$ CHO-A_{2B} and CHO-A_{2A}-A_{2B} cells. The one-way ANOVA with Dunnett's post-hoc test indicated significant differences. ns: not significant, $^{**}p < 0.01$, n = 2–4, see also Supplementary Table 4. The A_{2A}AR agonist CGS-21680 showed only a negligible signal in CHO-A_{2A}-A_{2B} cells at concentrations of up to 100 µM. (**B**) pK_B values for AR antagonists in cAMP accumulation assays in CHO-A_{2A}, CHO-A_{2B} and CHO-A_{2A}-A_{2B} cells with agonist stimulation by NECA. The one-way ANOVA with Dunnett's post-hoc test showed significant differences. ns: not significant, $^{**}p < 0.01$, n = 4–6, see also Supplementary Table 4. (**C**) pEC_{50} values of agonists and pK_B values of antagonists determined in cAMP accumulation assays at Jurkat-T cells (n = 3, see also Supplementary Table 4).

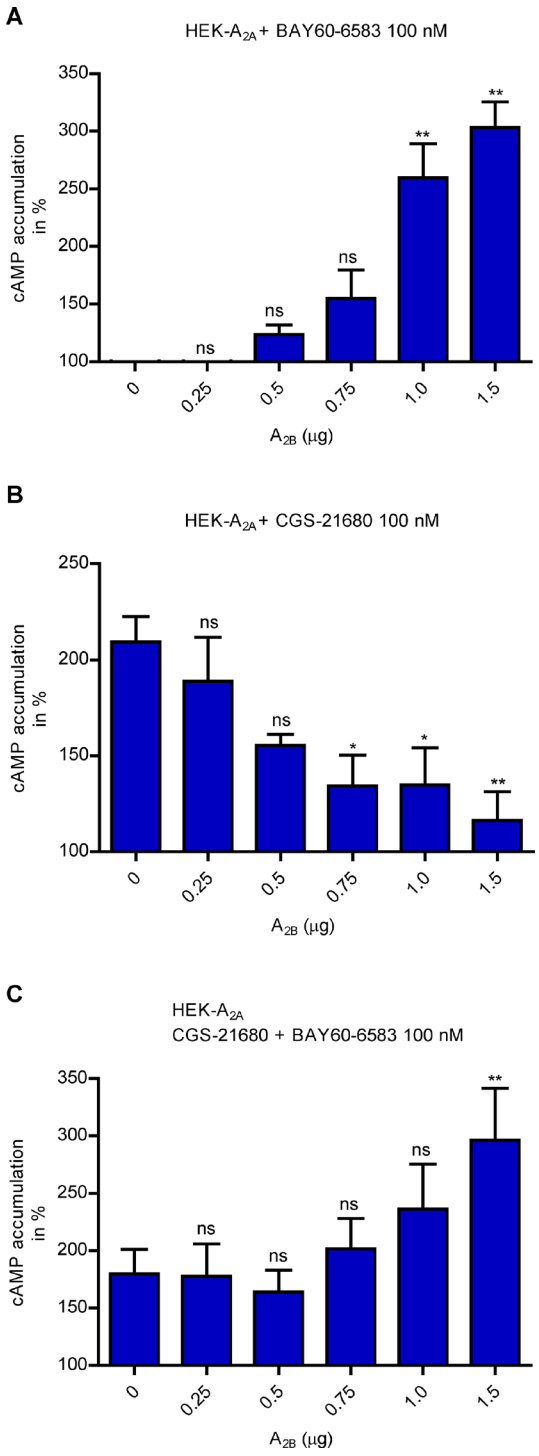

Figure 6: cAMP determination in cells coexpressing variable proportions of A_{2A} and A_{2B}ARs. (**A**) Stimulation of cAMP accumulation induced by 100 nM of the A_{2B}-selective partial agonist BAY60-6583 at HEK-A_{2A} cells transiently transfected with increasing amounts of cDNA for A_{2B}AR (0.25–1.5 µg). The basal cAMP level, i.e. HEK-A_{2A} cells only with medium but without the agonist, was set at 100%. The one-way ANOVA with Dunnett's post-hoc test showed significant differences. ns: not significant, $^{**}p < 0.01$ ($n = 2$, in triplicates). (**B**) Stimulation of cAMP accumulation induced by 100 nM of the A_{2A}-selective agonist CGS-21680 at HEK-A_{2A} cells transiently transfected with increasing amounts of cDNA for A_{2B}AR (0.25–1.5 µg). Basal cAMP, i.e. HEK-A_{2A} cells only with medium but without the agonist, was set at 100%. The one-way ANOVA with Dunnett's post-hoc test showed significant differences. ns: not significant, $^{*}p < 0.05$, $^{**}p < 0.01$ ($n = 2$, in triplicates). (**C**) Stimulation of cAMP accumulation induced by a combination of 100 nM of the A_{2A}-selective agonist CGS-21680 and of 100 nM of the A_{2B}-selective partial agonist BAY60-6583 at HEK-A_{2A} cells transiently transfected with with increasing amounts of cDNA for A_{2B}AR (0.25–1.5 µg). Basal cAMP, i.e. HEK-A_{2A} cells only with medium but without the agonist, was set at 100 %. The one-way ANOVA with Dunnett's post-hoc test showed significant differences. ns: not significant, $^{**}p < 0.01$ ($n = 2$, in triplicates).

through the A_{2B}AR (Figure 6B). Stimulation of the cells with a combination of both receptor subtype-selective agonists (100 nM each), showed a significant increase in cAMP accumulation with increasing amounts of transiently transfected A_{2B}AR additionally suggesting a dominant role for the A_{2B}AR (Figure 6C).

Dynamic mass redistribution assays

Finally, dynamic mass redistribution (DMR) assays providing a holistic readout were performed in HEK293T cells transiently transfected with different ratios of A_{2A} and A_{2B}AR cDNA. The A_{2B}-selective agonist BAY60-6583 (100 nM) displayed a time-dependent increase in the signal with increasing amounts of transiently transfected A_{2B}AR confirming the presence of functional A_{2B}ARs (Figure 7A). In contrast, when stimulating the cells with the A_{2A}-selective agonist, CGS21680 (100 nM), a time-dependent decrease in signal was observed with increasing amounts of transiently transfected A_{2B}AR suggesting an inhibition of the A_{2A}AR-mediated DMR signal through the A_{2B}ARs (Figure 7B). Stimulation of the cells with a combination of both, A_{2A} and A_{2B}AR agonist (100 nM each), showed a significant increase in signal with increased amounts of transiently transfected A_{2B}AR, but not with increased amounts of A_{2A}AR, additionally suggesting within the heteromer a dominant role for the A_{2B}AR (Figure 7C).

DISCUSSION

Adenosine is an important signaling molecule, and the A_{2A} and A_{2B}AR subtypes are established (A_{2A}) or potential (A_{2B}) drug targets. Both receptors are G_s protein-coupled, but the A_{2B}AR requires much higher adenosine concentrations to be activated than the A_{2A}AR, and its physiological role remains enigmatic. In the present study we demonstrate that A_{2B}ARs physically interact with A_{2A}ARs forming A_{2A}-A_{2B} heteromers. This interaction leads to new signalling properties as observed in cAMP experiments at Jurkat-T and further native and recombinant cells. Although A_1, A_{2A} and A_3 homomeric ARs and several heteromers of A_1 and A_{2A}ARs had previously been described [1, 40–41], neither homo- nor heteromers of A_{2B}ARs have been unambiguously demonstrated so far. Our study was motivated (i) by the fact that A_{2A} and A_{2B}ARs are frequently co-expressed; (ii) by the observation that A_{2A}AR pharmacology appears to be strikingly different than expected in a number of A_{2A}-A_{2B} co-expressing cells and tissues, (iii) by the still unknown physiological role of the "low-affinity" A_{2B}ARs; (iv) by contradictory results on pro- or anti-inflammatory effects mediated by the A_{2B}AR, and (v) by the observation that A_{2A} and A_{2B}ARs upon activation – although they are both G_s protein-coupled – often show opposite effects [25]. A_{2A}-A_{2B} heteromerization had previously been postulated to be required for high A_{2B}AR expression, and the C-terminus of the A_{2A}AR has been suggested to play an important role in this respect [42]. However, we could not confirm the published results. In fact, high A_{2B}AR expression is observed in many cancer cells including those which express lower amounts of A_{2A}ARs [12–13, 43–45]. Nevertheless, co-immunoprecipitation experiments on A_{2A}-A_{2B}AR-coexpressing HEK293 cells had provided the first indication of a possible existence of A_{2A}-A_{2B} heteromers [42]. In the present study, by applying several complementary techniques, we provide compelling evidence that A_{2A} and A_{2B} form heteromeric di-/oligomers in recombinant as well as in native cells and tissues. FRET experiments confirmed specific interaction between both receptor subtypes (Figure 1A). So far the structure of the heteromers and their interaction surface is still unknown. In the well-characterized A_{2A}-D_2 heteromer the long C-terminus of the A_{2A}AR is involved in heteromerization [46]. To gain insight into the A_{2A}-A_{2B} heteromer interface, we removed the C-terminus of the A_{2A}AR and examined the resulting truncated receptor mutant co-expressed with the A_{2B}AR in FRET experiments. The observed FRET signal was comparable to the one obtained for the wt A_{2A}-A_{2B}AR heteromer (Figure 1A, 1B) indicating that the C-terminus is not involved in the formation of A_{2A}-A_{2B} heteromers. Extensive BRET studies, including displacement experiments with untagged receptors, showed high, specific BRET signals for the A_{2A}-A_{2B}AR pair (Figure 2A, 2C). Incubation of cells with various agonists, adenosine (nonselective), NECA (nonselective), CGS-21680 (A_{2A}-selective), BAY60-6583 (A_{2B}-selective), or antagonists (PSB-603, A_{2B}-selective) did not lead to a significant change of the signal (Figure 2D). This means that A_{2A}-A_{2B} heteromer formation is independent of the presence of A_{2A} or A_{2B}AR ligands and stable in the presence of ligands. Furthermore BiFC experiments in which part of the EYFP sequence is attached to the A_{2A}, the other part to the A_{2B}AR, resulted in positive signals. These data convincingly underscore that both receptors are directly interacting, and that an A_{2A}-A_{2B} heterodi- or -oligomer must have been formed (Supplementary Figures 1, 2). A_{2A}-A_{2B} heteromer formation in CHO-A_{2A}-A_{2B} cells was confirmed by yet another technique, proximity ligation assays (PLA), using specific modified primary antibodies. The positive PLA signals obtained in living CHO-A_{2A}-A_{2B} cells, but not in non-transfected CHO cells, indicated close proximity of both receptors in the CHO cell line that coexpress them (Supplementary Figure 3). Thus, all conducted biophysical and biochemical techniques, namely FRET, BRET, BiFC and PLA studies, provided evidence that A_{2A} and A_{2B}ARs can form heteromers in living cells. Importantly, the existence of A_{2A}-A_{2B} heteromers in native tissues was confirmed by using the PLA approach (Figure 3, Supplementary Figures 4, 5) thus proving their physiological relevance. Remarkably, heteromers were detected in sections from hippocampus of the rat. Receptor

pharmacology was altered in cells expressing the two receptors and, therefore, also expressing A_{2A}-A_{2B} heteromers, as compared to that in cells expressing only one receptor subtype. This was initially observed in a recombinant system investigating CHO-A_{2A}, CHO-A_{2B} and CHO-A_{2A}-A_{2B} cells, the latter of which had higher A_{2B} than A_{2A}AR expression as assessed by RT-PCR and Western blot analysis. In cell lines only expressing A_{2A} or A_{2B}ARs, radioligand binding studies provided the expected affinities for standard ligands, i.e. high affinity binding of the selective A_{2A}AR ligands CGS-21680 (agonist) and MSX-2 (antagonist), but lacking affinity for the A_{2B}-selective

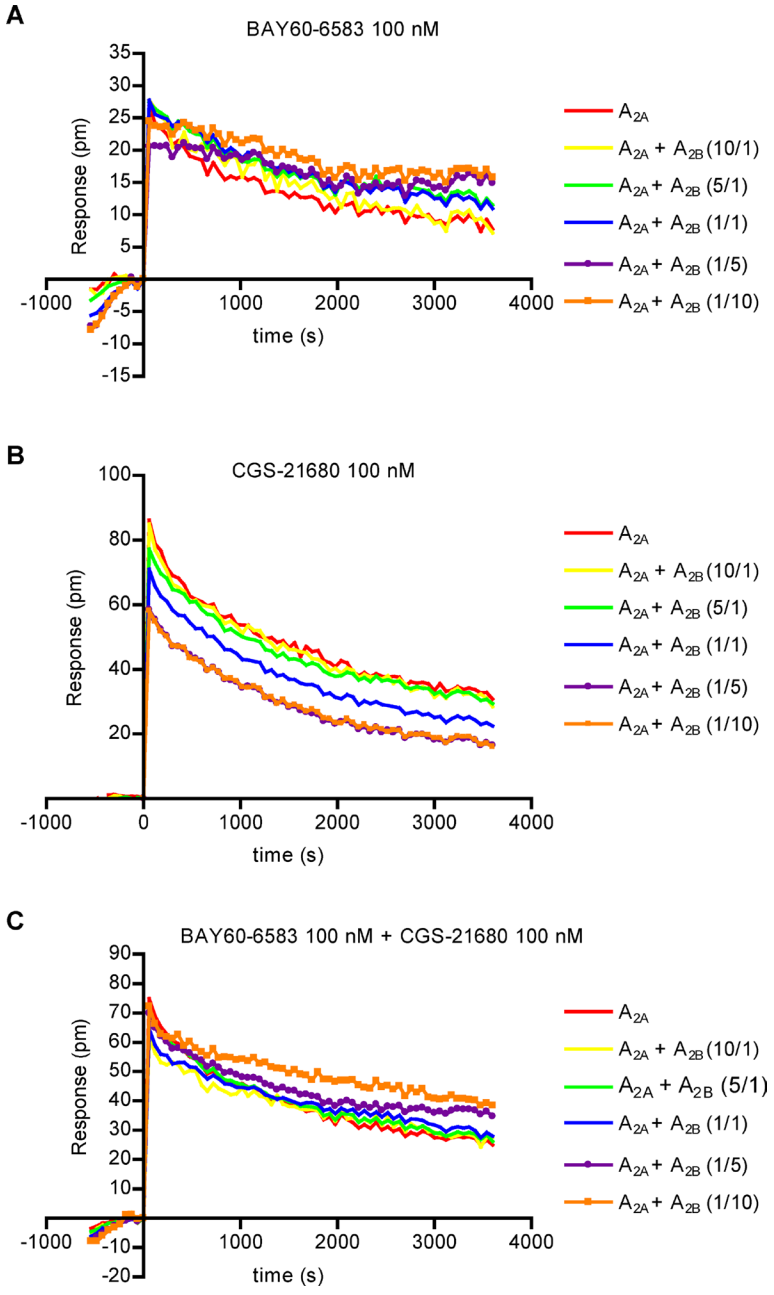

Figure 7: Label-free assays in cells coexpressing variable proportions of A_{2A} and A_{2B}ARs. (**A**) Time-dependent dynamic mass redistribution (DMR) measurement induced by 100 nM of the A_{2B}-selective partial agonist BAY60-6583 in HEK293T cells transiently transfected with a constant amount of cDNA for A_{2A}AR and increasing amounts of cDNA for A_{2B}AR, or *vice versa*, a constant amount of cDNA for A_{2B}AR and increasing amounts of cDNA for A_{2A}AR. (**B**) DMR measurement induced by 100 nM of the A_{2A}-selective agonist CGS-21680 in HEK293T cells transiently transfected with a constant amount of cDNA for A_{2A}AR and increasing amounts of cDNA for A_{2B}AR, or *vice versa*, a constant amount of cDNA for A_{2B}AR and increasing amounts of cDNA for A_{2A}AR. (**C**) DMR measurement induced by a combination of 100 nM of the A_{2A}-selective agonist CGS-21680 and of 100 nM of the A_{2B}-selective partial agonist BAY60-6583 at HEK293T cells transiently transfected with a constant amount of cDNA for A_{2A}AR and increasing amounts of cDNA for A_{2B}AR, or *vice versa*, a constant amount of cDNA for A_{2B}AR and increasing amounts of cDNA for A_{2A}AR.

ligands BAY60-6583 (partial agonist) and PSB-603 (antagonist) at the CHO-A_{2A} cells and *vice versa* for the CHO-A_{2B} cells (Supplementary Tables 2, 3). At the CHO-A_{2A}-A_{2B} cell line, however, no binding for the A_{2A}-selective radioligands [^{3}H]MSX-2 and [^{3}H]CGS-21680 was detected although we could clearly prove both the presence of A_{2A}AR mRNA and A_{2A}AR protein in this cell line (Supplementary Figures 8A, 8B, 6A, 6B, Supplementary Table 2) and its cell surface localization (Supplementary Figure 3C). The A_{2A}-A_{2B} heteromer behaved almost like an A_{2B}AR by displaying low affinity for adenosine and NECA (Figure 4A, 4B), high affinity for PSB-603 and no significant sign of A_{2A}AR activation. cAMP accumulation assays yielded results in line with the pharmacology obtained in binding studies (Figure 5A–5C, Supplementary Table 4). Moreover in cAMP assays as well as in DMR assays at HEK-A_{2A} cells transiently transfected with increasing amounts of the A_{2B}AR (Figure 6A–6C, Figure 7A–7C) a clear inhibiton of A_{2A}AR function through A_{2B}ARs could be demonstrated. This means that the A_{2A}AR signaling appears to be completely blocked in the A_{2A}-A_{2B} heteromer. On a molecular level, this would mean that the A_{2B}AR modulates the conformation of the binding site of the A_{2A}AR in such a way that it either loses its affinity for ligands completely, and only the A_{2B} binding site is available for interaction with ligands, or the A_{2A} binding site in the heteromer switches to A_{2B}-like properties. Both would in principle be possible. In fact, the binding sites for adenosine in A_{2A} and A_{2B}ARs are almost identical differing only in a single amino acid (A_{2A}: L249, A_{2B}: V250), and yet their affinity for adenosine is very different. It is therefore likely that the ligand binding site of A_{2A} and A_{2B}ARs is readily amenable to allosteric modulation. The discovery of A_{2A}AR action blockade by the A_{2B}AR was very consistent when assayed in heterologous expression systems, in cell lines or in primary cells. Other groups had previously confirmed A_{2A} and A_{2B} mRNA expression in Jurkat-T cells ($A_{2B} \geq A_{2A}$) and discovered that the selective A_{2A}AR agonist CGS-21680 was nearly inactive in cAMP assays [47], and also the binding of [^{3}H]CGS-21680 (12.5 nM) to Jurkat-T cell membranes was found to be negligible [48]. These results can now be explained by taking into account our discovery that the A_{2A}AR is non-functional within the A_{2A}-A_{2B} heteromer context present in Jurkat-T cells. Our findings also provide a mechanistic basis to interpret previous results, namely the altered AR pharmacology in cells expressing both A_{2B} and A_{2A}ARs with similar or higher levels of A_{2B} ($A_{2B} \geq A_{2A}$). In Supplementary Table 5 we have collected the appropriate literature data that may now be interpreted in the light of our main finding. For example, in the human bladder carcinoma cell line T24 the expression of A_{2B} and A_{2A} receptors was demonstrated by RT-PCR ($A_{2B} > A_{2A}$). In cAMP assays NECA and adenosine were able to induce cAMP accumulation whereas the A_{2A}-selective agonist CGS-21680 was inactive [45]. Wei *et al*. showed expression of all four AR subtypes in three prostate cancer cell lines by qRT-PCR and Western blot experiments, with domination of the A_{2B}AR ($A_{2B} > A_{2A}$). NECA and the selective A_{2B}AR agonist BAY60-6583, but not the A_{2A}-selective agonist CGS-21680, concentration-dependently induced cAMP accumulation [13]. Recently, Hajiahmadi *et al*. demonstrated expression of all four AR subtypes in three human ovarian cancer cell lines by qRT-PCR and Western blot, in which, again, the A_{2B}AR was the most abundant one ($A_{2B} > A_{2A}$), and NECA but not the A_{2A}AR agonist CGS-21680, concentration-dependently induced cAMP accumulation [12]. In contrast, in A_{2A}-A_{2B}-co-expressing cell lines and tissues in which the expression level of A_{2A}ARs is higher than that of A_{2B} ($A_{2A} > A_{2B}$), e.g. in T-lymphocytes from human blood, PC12 cells, or HMC-1 cells, canonical A_{2A} and A_{2B} pharmacology is observed (Supplementary Tables 2, 5) [8, 16, 49–50]. It is likely that A_{2A}-A_{2B}AR heteromers exist in these cells but in a proportion that does not prohibit activation of *free* A_{2A}ARs (that cannot be blocked by A_{2B}ARs). Thus, regulation of A_{2A} and A_{2B} expression levels can in turn govern the pharmacological outcome of stimulation with adenosine or synthetic AR agonists. Both G_s-coupled A_2AR subtypes play important (patho)physiologic roles and are co-expressed on many cell types and tissues [6, 8, 11, 51]. Up-regulation of A_{2A}AR expression in different tissues can be found under various pathological conditions. For example, lymphocytes from amyotrophic lateral sclerosis (ALS) or multiple sclerosis (MS) patients show increased A_{2A}AR levels [16–17]. NF-kappaB was found to enhance hypoxia-driven T-cell immunosuppression via activation of upregulated A_{2A}ARs [52]. In a study on isolated perfused mouse heart investigating the contributions of A_{2A} and A_{2B}ARs on cardiac flow, the A_{2A}-selective agonist CGS-21680 and the non-selective agonist NECA increased coronary flow in A_{2B} knockout (KO) mice to a significantly higher degree than in wildtype (WT) mice [51]. The A_{2A}-selective antagonist SCH58261 blocked NECA-induced increase in coronary flow to a higher degree in KO than in WT mice. The authors explained these discrepancies by an observed upregulation of A_{2A}ARs (ca. 20% as estimated by Western blot) in mesenteric arterioles of KO as compared to WT mice. However, an additional or alternative explanation could be that by deletion of A_{2B}ARs, heteromer formation would no longer be possible leading to a de-blocking of the A_{2A}ARs and thus a higher number of free receptors with typical A_{2A} pharmacology. Several studies have led to the proposal that GPCR heteromers may constitute drug targets in their own right and that heteromers can be upregulated in disease [53]. It appears that A_{2A} and A_{2B}ARs display very high affinity for each other, and whenever they are co-expressed they would form stable heteromers with a distinct pharmacology. This implies that the A_{2A}-A_{2B} interface and the interactions must be unique to produce such a remarkable and persistent disappearance of A_{2A}AR ligand recognition and signaling through allosteric receptor-receptor modulation.

MATERIALS AND METHODS

Molecular biology

For FRET experiments the cDNAs of the human A_{2A}AR and the C-terminal truncated mutant A_{2A}1-293R were amplified by PCR using primers that delete the stop codon of the receptors and introduce *EcoRI* and *AgeI* restriction enzyme sites. The resulting PCR products were cloned in-frame with *EcoRI/AgeI* into the vectors pEYFP-N1 and pGFP²-N3, respectively. The cDNA of the human A_{2B}AR was also cloned with *EcoRI/AgeI* into the vector pGFP²-N3. For a positive control a fusion protein GFP²-EYFP was used. The cDNA of GFP² was amplified by PCR using primers that delete the stop codon of the protein and introduce *BamHI* and *AgeI* restriction enzyme sites. The resulting PCR product was cloned in-frame with *BamHI/AgeI* into pEYFP-N1 plasmid, respectively. The cDNA of the $GABA_B$R2-EYFP receptor construct was a gift from Prof. Franco. For BRET experiments the cDNAs of the human A_{2A} and A_{2B}AR were amplified by PCR using primers that delete the stop codon of the receptors and introduce *EcoRI* and *BamHI* restriction enzyme sites. The resulting A_{2A} and A_{2B}AR PCR products were cloned in-frame with *EcoRI/BamHI* into pRluc-N2. The dopamine D_2-pRluc-N2 receptor construct was a gift from Prof. Franco. The A_{2A}AR cDNA was cloned in-frame with *EcoRI/AgeI* into pEYFP-N1, respectively. For BRET experiments *Rluc*-EYFP was used as a positive control, and *Rluc* alone and EYFP plasmids alone were employed as negative controls. For the positive control the cDNA of *Rluc* was amplified by PCR using primers that delete the stop codon of the protein and introduce *EcoRI* and *BamHI* restriction sites. The resulting PCR product was cloned in-frame with *EcoRI/BamHI* into pEYFP-N1 plasmid, respectively. For BRET displacement experiments, the cDNA of the human A_{2B}AR was cloned with *EcoRI/NotI* into the pcDNA3.1(+) plasmid.

Transiently transfected HEK293T cells were prepared by subcloning the cDNAs of the human A_{2A} and A_{2B}AR with *HindIII/BamHI* into the vector pcDNA3.1(+). All restriction enzymes and supplements for the molecular biology were obtained at NEB (Frankfurt, Germany). DNA and RNA purification kits were obtained at Zymo Research (Freiburg, Germany) or Life Technologies GmbH (Darmstadt, Germany).

Transient transfection of CHO-K1 cells for FRET and BRET experiments

For FRET and BRET experiments CHO-K1 cells were transiently co-transfected with constant amounts of the receptor-donor DNA (e.g. A_{2B}-GFP² or A_{2B}-*Rluc*) and constant or increasing amounts of receptor-acceptor DNA (e.g. A_{2A}-EYFP) using Lipofectamine 2000 (Thermo Fisher Scientific, Waltham, USA). Moreover the receptor-donor DNAs and receptor-acceptor DNAs were transfected alone to determine their contribution to the detection channels (spectral signature). The cells were harvested 24 h after transfection and used for FRET, and BRET experiments, respectively.

FRET experiments analyzed by fluorimetry

FRET experiments were conducted as previously described [36]. 20 µg of the transfected cells (100 µl) were distributed in duplicates in a black 96-well plate with black bottom for fluorescence measurements. The fluorescence signals were detected by a Mithras LB 940 fluorimeter using a 10-nm bandwidth excitation filter at 405 nm and 500 nm and 10-nm bandwidth and 25-nm bandwidth emission filters corresponding to 510 nm and 535 nm (GFP² exication 405 nm, emission 510 nm; EYFP exication 500 nm, emission 535 nm). Background fluorescence signals from non-transfected CHO-K1 cells were substracted. For all experiments the gain settings and the read time of 0.1 s were kept identical.

Quantification of FRET signal

Quantification of the FRET signals was performed as described by Elder *et al*. according to a sensitized emission method [54]. This method requires correction for donor bleed-through (donor fluorophore emission into the acceptor channel) and acceptor cross-excitation (direct excitation of acceptor fluorophores by donor excitation). For that, the contributions of GFP² and EYFP proteins alone to the two detection channels were measured in experiments with cells expressing only one of these proteins. The spectral signatures of the different receptors fused to either GFP² or EYFP did not significantly vary from the determined spectral signatures of the fluorescent proteins alone. The donor bleed-through correction factor (DER, measured in cells expressing only donor fluorophors) and acceptor cross-excitation factor (AER, measured in cells expressing only acceptor fluorophores) were calculated using the following formula [54]:

$$AER = \frac{I^{DA}}{I^{AA}} \quad DER = \frac{I^{DA}}{I^{DD}}$$

The AER is the ratio of emission into the acceptor channel when using donor excitation relative to when using acceptor excitation. The DER is the ratio of emission into the acceptor channel relative to emission into the donor channel, when using donor excitation [54]. The corrected FRET signal was then calculated according to the following formula [54]:

$$cFRET = I^{DA} - DER * I^{DD} - AER * I^{AA}$$

Different FRET normalisation equations can be used to determine the efficiency of the FRET signal.

Here we used the N_{FRET} normalizing method according to Shyu *et al.,* which takes changes in donor and acceptor concentrations into account [55]:

$$N_{FRET} = \frac{cFRET}{\sqrt{(I^{DD} * I^{AA})}}$$

FRET signal analyses were done in Excel and results were displayed using GraphPad Prism 4.

Bioluminescence resonance energy transfer (BRET) experiments analyzed by fluorimetry

BRET experiments were conducted as previously described [36]. 20 µg of the transfected cells (100 µl) were distributed in duplicates into a black 96-well plate with black bottom for fluorescence and a white 96-well plate with white bottom for bioluminescence measurements. Signals were detected by a Mithras LB 940 fluorimeter calculating the integration for bioluminescence using filters for 440–500 nm (485 nm maximum emission of bioluminescence), and for fluorescence with a filter for 510–590 nm (530 nm maximum emission of EYFP). To confirm equal expression of Rluc and increasing expression of EYFP, for each sample bioluminescence and fluorescence was measured before starting the experiment. EYFP fluorescence was defined as the fluorescence of the sample minus the fluorescence of cells expressing only *Rluc*-tagged receptors. For BRET, 5 µM coelenterazine-H (PJK, Kleinblittersdorf, Germany) was added to the samples and measurements were performed after 1 min (net BRET determination) and after 10 min (*Rluc* luminescence quantification). Net BRET was defined as the bioluminescence of the sample minus the bioluminescence of cells expressing only *Rluc*-tagged receptors. BRET signals were determined by calculating the ratio of the light emitted by EYFP over the light emitted by the *Rluc A*. milliBRET unit (mBU) is the BRET ratio × 1000. Curves were fitted using nonlinear regression. Displacement studies were performed in triplicates at a constant BRET ratio, around the $BRET_{50}$ of the A_{2B}AR-Rluc/A_{2A}AR-YFP pair, and increasing amounts of the A_{2B}AR. For testing the effects of compounds on heteromerization of A_{2A}AR and A_{2B}AR the agonists adenosine (100 µM), NECA (100 µM), CGS-21680 (A_{2A}R, 10 µM), BAY60-6583 (A_{2B}R, 10 µM), and the antagonist PSB-603 (A_{2B}R, 500 nM) were added for 60 min to cells which expressed A_{2B}AR-Rluc and A_{2A}AR-YFP, around the $BRET_{50}$ value. The final DMSO concentration in these experiments was 2.5 % and experiments were performed in triplicates.

In situ proximity ligation assay in the rat brain

The experiments were carried out in accordance with the European Directive 2010/63/EU and were approved by the Bioethical Committee at Karolinska Institutet. Male Sprague-Dawley (derived from the licensed animal breeder Charles River, Sulzfeld, Germany), weighing between 260–310 g at the beginning of the experiment, were used. The animals (n = 5) were housed individually in standard plastic rodent cages (25 cm × 30 cm × 30 cm) in a colony room maintained at 21 ± 1° C and 40–50 % humidity under a 12-hour light-dark cycle (lights on at 6:00 am). Rodent food and water were available *ad libitum*. All animals used for the *in situ* PLA neurochemical study were experimentally naive.

To study the distribution of the adenosine A_{2A}-A_{2B} heteroreceptor complex in the rat brain the *in situ* proximity ligation assay (*in situ* PLA) was performed as described previously [56].

Retroviral transfection

CHO cells stably expressing HA-tagged human A_{2A} or A_{2B}ARs, or both human A_{2A} and A_{2B}ARs were generated using a retroviral transfection system [5]. HeLa cells stably overexpressing HA-tagged human A_{2A}ARs were also generated using a retroviral transfection system [5]. For generating the A_{2A}-A_{2B} co-expressing cell line, GP^{+}env AM12 cells were co-transfected with 6.75 µg of the pQCXIP-A_{2A} vector construct and 3.25 µg of VSV-G using Lipofectamine 2000. The supernatant medium containing the modified virus was filtered and transferred into a small flask of 70% confluent CHO-A_{2B} cells. After infection the selection of the CHO-A_{2A}-A_{2B} cells was started after 48 h by the addition of 10 µg/ml of puromycin.

Cell culture

Chinese hamster ovary cells (CHO-K1), GP^{+} env AM12 cells and CHO cells stably expressing human A_{2A}ARs, HA-tagged human A_{2A}AR or human A_{2B}AR were cultured as drecribed previously [5, 57]. CHO cells stably co-transfected with human A_{2A}AR and A_{2B}AR were maintained in Dulbecco's Modified Eagle Medium (DMEM-F12) medium supplemented with 10% (v/v) fetal calf serum (FCS), 100 units/ml penicillin, 100 µg/ml streptomycin, 800 µg/ml G418 and 10 µg/ml puromycin at 37° C and 5 % CO_2. Human Jurkat-T cells natively expressing A_{2A} and A_{2B}ARs were cultured in RPMI 1640 medium supplemented with 10 % (v/v) fetal calf serum (FCS), 100 units/ml penicillin, 100 µg/ml streptomycin and 2 mM *L*-glutamine. HeLa cells natively expressing human A_{2A} and A_{2B}ARs were cultured in DMEM supplemented with 10% (v/v) FCS, 100 units/ml penicillin, 100 µg/ml streptomycin. HeLa cells stably overexpressing the human HA-tagged A_{2A}AR were cultured in the same medium with the addition of 800 µg/ml of G418. HEK293T cells were grown in DMEM supplemented with 2 mM *L*-glutamine, 5% (v/v) FCS, 100 units/ml penicillin, 100 µg/ml streptomycin, and

minimal essential medium non-essential amino acid solution (1:100) at 37° C in an atmosphere of 5 % CO_2. All cell culture media and supplements were obtained from (Darmstadt, Germany), Sigma-Aldrich (Munich, Germany) or Applichem (Darmstadt, Germany).

Membrane preparation

The preparations of CHO and HeLa membranes recombinantly (or natively) expressing human A_{2A} and/or A_{2B}AR subtypes were performed as previously described [5]. Membranes from HEK-A_{2B} or A_{2A} cells, which were used for some of the radioligand competition binding studies, were purchased from Perkin Elmer (Waltham, USA). The preparation of Jurkat-T cell membranes was performed as follows: a Jurkat-T cell suspension was centrifuged in 50 ml falcon tubes at 200 g, 4° C, 5 min. The supernatant was discarded and the cell pellets were quickly frozen at –80° C. The defrosted pellets were then resuspended in ice-cold 25 mM Tris-buffer, 0.32 M sucrose, 1 mM ethylenediaminetetraacetic acid (EDTA), 0.1 mM phenylmethanesulfonylfluoride (PMSF), pH 7.4, and homogenized with an Ultra-Turrax (30 s on ice). The homogenate was centrifuged for 10 min at 1000 *g* at 4° C. The resulting pellets were discarded and the supernatant was centrifuged for 1 h at 48.000 g at 4° C. Pellets containing the membranes were resuspended in aqua bidest., homogenized with an Ultra-Turrax (30 s on ice) and centrifuged under the same conditions. The supernantant was discarded and the pellets were resuspended in 50 mM Tris-buffer, pH 7.4 and homogenized with a glass Teflon homogenizer on ice. The resuspended and homogenzied pellets were aliquoted and stored at –80° C until use. The protein content of all membrane preparations was determined with the Lowry method [58].

Radioligand binding assays

Radioligand receptor binding experiments at membrane preparation of native (HeLa) and recombinant cells (CHO- or HEK cells recombinantly expressing A_{2A} and/or A_{2B}ARs) using the A_{2B}-selective antagonist radioligand [^{3}H]PSB-603 (spec. activity: 79 Ci/mmol) to detect A_{2B}ARs were performed as previously described [59]. Competition binding experiments at various membrane preparations of native (HeLa, Jurkat-T) and recombinant cells (CHO or HEK cells expressing A_{2A} and/or A_{2B}ARs) using the A_{2A}-selective antagonist radioligand [^{3}H]MSX-2 (spec. activity: 85 Ci/mmol) to detect A_{2A}ARs were performed in analogy to described procedures [39]. The assay was performed in a final volume of 400 µl containing 4 µl of test compound dissolved in DMSO, 196 µl buffer (50 mM Tris-HCl, pH 7.4), 100 µl of radioligand solution in the same buffer (1 nM), and 100 µl of membrane preparation (10 to 200 µg protein per vial, 2 U/ml adenosine deaminase (ADA) 20 min incubation at rt). Non-specific binding was determined in the presence of unlabeled MSX-2, or CGS-15943, respectively (10 µM), both giving identical results.

Competition binding experiments at membrane preparations of native cells (HeLa, Jurkat-T cells) or recombinant cells (CHO, HEK or HeLa recombinantly expressing the human A_{2A}AR) using the agonist radioligand [^{3}H]CGS-21680 (spec. activity: 39 Ci/mmol) were performed in analogy to described procedures [5]. The assay was performed in a final volume of 400 µl containing 4 µl of test compound dissolved in DMSO, 196 µl buffer (50 mM Tris-HCl, 10 mM $MgCl_2$ pH 7.4), 100 µl of radioligand solution in the same buffer (5 nM), and 100 µl of membrane preparation (10 to 200 µg of protein per vial, 2 U/ml ADA 20 min incubation at rt). Non-specific binding was determined in the presence of NECA (10 or 50 µM, respectively) or CGS-15942 (final concentration 10 µM); all gave identical results. All data were analyzed with GraphPad Prism, Version 4 (GraphPad Inc., La Jolla, CA).

Radioligand binding assays at Jurkat-T cell membranes

Competition binding experiments at Jurkat-T cell membrane preparations using the A_{2B}-selective antagonist radioligand [^{3}H]PSB-603 to detect A_{2B}ARs were performed in a final volume of 1000 µl containing 25 µl of test compound dissolved in DMSO/50 mM Tris-buffer pH 7.4 (1:1), 375 µl of assay buffer (50 mM Tris-HCl, pH 7.4), 100 µl of radioligand solution in the same buffer (final concentration 0.3 nM), and 500 µl of membrane suspension (100–200 µg protein per vial, 2 U/ml 20 min incubation at rt). Non-specific binding was determined in the presence of unlabeled PSB-603 (10 nM) or DPCPX (10 µM); both gave similar results. After an incubation time of 60 min at rt, the assay mixture was filtered through GF/B glass fiber filters. Washing buffer: 50 mM Tris-HCl buffer, 0.1% bovine serum albumin (BSA), pH 7.4.

cAMP assays

The determination of cAMP accumulation in recombinant CHO and in Jurkat-T cells was performed as previously described [5, 60]. K_B-values for the A_{2A}-specific antagonist MSX-2, the A_{2B}-specific antagonist PSB-603 and the non-selective antagonist caffeine were determined versus the full agonist NECA. K_B-values were calculated using the child equation [61].

Transient transfection of HEK293T cells for cAMP assays

HEK293T cells were transiently transfected with the corresponding cDNA (pcDNA3.1+-hA_{2B}, pcDNA3.1+-

hA_{2A}) by the polyethylenimine (Sigma) method [62]. The determination of AR-induced cAMP accumulation in HEK293T cells transiently expressing A_{2A} and A_{2B}ARs was performed as previously described [62].

Dynamic mass redistribution assays

Dynamic mass redistribution (DMR) at HEK293T cells transfected with A_{2A} and A_{2B}ARs was determined as described previously [62]. In brief, 24 h before the assay, cells were seeded at a density of 7,500 cells per well in 384-well sensor microplates with 40 µl of growth medium and cultured for 24 h (37° C, 5 % CO_2) to obtain 70–80% confluent monolayers. Prior to the assay, cells were washed twice with assay buffer (Hank's balanced salt solution; HBSS with 20 mM HEPES, pH 7.15) and incubated for 2 h in 40 µl per well of assay buffer in the DMR reader at 24° C. Hereafter, the sensor plate was scanned and a baseline optical signature was recorded before adding 10 µl of test compound dissolved in assay buffer containing 0.1% DMSO and DMR responses were monitored for at least 8,000 s using an EnSpire® Multimode Plate Reader (PerkinElmer, Waltham, MA, USA) by a label-free technology. Data were analyzed using EnSpire Workstation Software v 4.10.

Abbreviations

ADA: adenosine deaminase; AR: adenosine receptor(s); BAY60-6583: 2-({6-amino-3,5-dicyano-4-[4-(cyclopropylmethoxy)phenyl]pyridin-2-yl}sulfanylacetamide; BiFC: bimolecular fluorescence complementation; BRET: bioluminescence resonance energy transfer; BSA: bovine serum albumin; cDNA: complementary deoxyribonucleic acid; CGS-21680: (2-*p*-[2-carboxyethyl]phenethylamino)-5′-*N*-ethylcarboxamidoadenosine; CHO: Chinese hamster ovary; DAPI: 4′,6-diamidin-2-phenylindole; DEPC: diethylpyrocarbonate; DMEM: Dulbecco's Modified Eagle Medium; DMSO: dimethylsulfoxide; DPCPX: 8-cyclopentyl-1,3-dipropylxanthine; DMR: dynamic mass redistribution; EDTA: ethylenediamine tetraacetic acid; EGTA: ethyleneglycoltetraacetic acid; EYFP: enhanced yellow fluorescent protein; FCS: fetal calf serum; FRET: Förster resonance energy transfer; GFP^2: green fluorescent protein variant 2; GPCR: G protein-coupled receptor; G418: geneticin; HA: human influenza hemagglutinin tag; h: human; HBSS: Hank's balanced salt solution; KO: knock-out; KRH: Krebs-Ringer-Hepes; mRNA: messenger ribonucleic acid; MSX-2: 3-(3-hydroxypropyl)-7-methyl-8-(*m*-methoxystyryl)-1-propargylxanthine; NECA: 5′-*N*-ethylcarboxamidoadenosine; PBS: phosphate buffered saline; PEI: polyethylenemine; PMSF: phenylmethanesulfonyl fluoride; PVDF: polyvinylidene fluoride; PSB-603: 8-(4-(4-(4-chlorophenyl)-piperazine-1-sulfonyl)phenyl)-1-propylxanthine; Rluc: Renilla Luciferase; RNA: ribonucleic acid; Ro 20-1724: 4-(3-butoxy-4-methoxyphenyl)methyl-2-imidazolidone; RPMI: Roswell Park Memorial Institute; rt: room temperature; RT-PCR: reverse transcriptase-polymerase chain reaction; TBS: Tris buffered saline; Tris: Tris(hydroxymethyl)aminomethan.

Author contributions

SH designed, performed and analyzed FRET and BiFC experiments, cloned some of the receptor constructs for BRET experiments, prepared the stably transfected CHO-A_{2B}, CHO-A_{2A}-A_{2B} cell lines and characterized them and performed the majority of radioligand binding and cAMP assays. GN designed, performed and interpreted the DMR studies and cAMP experiments at HEK-A_{2A} cells. DBE designed, performed and analyzed PLA experiments at rat brains; YCA established and performed PLA experiments at CHO-A_{2A}-A_{2B} cells, performed Western blots at CHO-A_{2A}-A_{2B} and Jurkat-T cell membranes and analyzed results. BFS and BC designed, performed and analyzed BRET experiments. AD, EdF and MR prepared some of the stably transfected cell lines, characterized them and performed and analyzed cAMP experiments. SKL performed radioligand binding studies at human T-lymphocytes and analyzed the results. ACS designed PLA experiments at the CHO-A_{2A}-A_{2B} cell line and supervised some of the molecular biology studies. CEM, SH and RF wrote the manuscript; GN, DBE and KF contributed to writing the manuscript. RF designed and supervised some of the FRET, BRET and DMR studies. CEM designed and supervised the complete study.

ACKNOWLEDGMENTS

We thank Prof. Dr. Tom Kerppola for providing the Jun and Fos cDNA constructs. Angelika Fischer and Anika Püsche are acknowledged for expert technical assistance. We thank Magdalena Navarro Sala for performing some BRET and FRET experiments and Anna Werning for the cloning of some of the receptor constructs. Barbora Červinková is grateful to the European Commission for support within the Erasmus program.

CONFLICTS OF INTEREST

The authors declare no competing or financial interest.

REFERENCES

1. Fredholm BB, IJzerman AP, Jacobson KA, Linden J, Müller CE. International Union of Basic and Clinical Pharmacology. LXXXI. Nomenclature and classification of adenosine receptors-an update. Pharmacol Rev. 2011; 63:1–34.
2. Abbracchio MP, Brambilla R, Ceruti S, Kim HO, von Lubitz DK, Jacobson KA, Cattabeni F. G protein-dependent

activation of phospholipase C by adenosine A_3 receptors in rat brain. Mol Pharmacol. 1995; 48:1038–1045.

3. Linden J, Thai T, Figler H, Jin X, Robeva AS. Characterization of human $A_{(2B)}$ adenosine receptors: radioligand binding, western blotting, and coupling to $G_{(q)}$ in human embryonic kidney 293 cells and HMC-1 mast cells. Mol Pharmacol. 1999; 56:705–713.
4. Fredholm BB, IJzerman AP, Jacobson KA, Klotz KN, Linden J. International Union of Pharmacology. XXV. Nomenclature and classification of adenosine receptors. Pharmacol Rev. 2001; 53:527–552.
5. De Filippo E, Namasivayam V, Zappe L, El-Tayeb A, Schiedel AC, Müller CE. Role of extracellular cysteine residues in the adenosine A_{2A} receptor. Purinergic Signal. 2016; 12:313–329.
6. Chandrasekera PC, McIntosh VJ, Cao FX, Lasley RD. Differential effects of adenosine A_{2A} and A_{2B} receptors on cardiac contractility. Am J Physiol Heart Circ Physiol. 2010; 299:H2082–2089.
7. Morello S, Pinto A, Blandizzi C, Antonioli L. Myeloid cells in the tumor microenvironment: Role of adenosine. Oncoimmunology. 2016; 5:e1108515.
8. Schiedel AC, Lacher SK, Linnemann C, Knolle PA, Müller CE. Antiproliferative effects of selective adenosine receptor agonists and antagonists on human lymphocytes: evidence for receptor-independent mechanisms. Purinergic Signal. 2013; 9:351–365.
9. Johnston-Cox HA, Ravid K. Adenosine and blood platelets. Purinergic Signal. 2011; 7:357–365.
10. Gnad T, Scheibler S, von Kügelgen I, Scheele C, Kilic A, Glode A, Hoffmann LS, Reverte-Salisa L, Horn P, Mutlu S, El-Tayeb A, Kranz M, Deuther-Conrad W, et al. Adenosine activates brown adipose tissue and recruits beige adipocytes via A_{2A} receptors. Nature. 2014; 516:395–399.
11. Kalhan A, Gharibi B, Vazquez M, Jasani B, Neal J, Kidd M, Modlin IM, Pfragner R, Rees DA, Ham J. Adenosine A_{2A} and A_{2B} receptor expression in neuroendocrine tumours: potential targets for therapy. Purinergic Signal. 2012; 8:265–274.
12. Hajiahmadi S, Panjehpour M, Aghaei M, Mousavi S. Molecular expression of adenosine receptors in OVCAR-3, Caov-4 and SKOV-3 human ovarian cancer cell lines. Res Pharm Sci. 2015; 10:43–51.
13. Wei Q, Costanzi S, Balasubramanian R, Gao ZG, Jacobson KA. A_{2B} adenosine receptor blockade inhibits growth of prostate cancer cells. Purinergic Signal. 2013; 9:271–280.
14. Chen JF, Eltzschig HK, Fredholm BB. Adenosine receptors as drug targets-what are the challenges? Nat Rev Drug Discov. 2013; 12:265–286.
15. Batalha VL, Ferreira DG, Coelho JE, Valadas JS, Gomes R, Temido-Ferreira M, Shmidt T, Baqi Y, Buee L, Müller CE, Hamdane M, Outeiro TF, Bader M, et al. The caffeine-binding adenosine A_{2A} receptor induces age-like HPA-axis dysfunction by targeting glucocorticoid receptor function. Sci Rep. 2016; 6: 31493.
16. Vincenzi F, Corciulo C, Targa M, Casetta I, Gentile M, Granieri E, Borea PA, Popoli P, Varani K. A_{2A} adenosine receptors are up-regulated in lymphocytes from amyotrophic lateral sclerosis patients. Amyotroph Lateral Scler Frontotemporal Degener. 2013; 14:406–413.
17. Vincenzi F, Corciulo C, Targa M, Merighi S, Gessi S, Casetta I, Gentile M, Granieri E, Borea PA, Varani K. Multiple sclerosis lymphocytes upregulate A_{2A} adenosine receptors that are antiinflammatory when stimulated. Eur J Immunol. 2013; 43:2206–2216.
18. Linden J, Cekic C. Regulation of lymphocyte function by adenosine. Arterioscler Thromb Vasc Biol. 2012; 32:2097–2103.
19. Eckle T, Kewley EM, Brodsky KS, Tak E, Bonney S, Gobel M, Anderson D, Glover LE, Riegel AK, Colgan SP, Eltzschig HK. Identification of hypoxia-inducible factor HIF-1α as transcriptional regulator of the A_{2B} adenosine receptor during acute lung injury. J Immunol. 2014; 192:1249–1256.
20. Yang M, Ma C, Liu S, Shao Q, Gao W, Song B, Sun J, Xie Q, Zhang Y, Feng A, Liu Y, Hu W, Qu X. HIF-dependent induction of adenosine receptor A_{2B} skews human dendritic cells to a Th2-stimulating phenotype under hypoxia. Immunol Cell Biol. 2010; 88:165–171.
21. Feoktistov I, Ryzhov S, Zhong H, Goldstein AE, Matafonov A, Zeng D, Biaggioni I. Hypoxia modulates adenosine receptors in human endothelial and smooth muscle cells toward an A_{2B} angiogenic phenotype. Hypertension. 2004; 44:649–654.
22. Sitkovsky M, Lukashev D, Deaglio S, Dwyer K, Robson SC, Ohta A. Adenosine A_{2A} receptor antagonists: blockade of adenosinergic effects and T regulatory cells. Br J Pharmacol. 2008; 153:S457–464.
23. Müller CE, Stein BS. Adenosine receptor antagonists: structures and potential therapeutic applications. Curr Pharm Des 1996; 2:502–530.
24. Sepulveda C, Palomo I, Fuentes E. Role of adenosine A_{2B} receptor overexpression in tumor progression. Life Sci. 2016; 166:92–99.
25. Feoktistov I, Biaggioni I. Role of adenosine $A_{(2B)}$ receptors in inflammation. Adv Pharmacol. 2011; 61:115–144.
26. Ferré S, Baler R, Bouvier M, Caron MG, Devi LA, Durroux T, Fuxe K, George SR, Javitch JA, Lohse MJ, Mackie K, Milligan G, Pfleger KD, et al. Building a new conceptual framework for receptor heteromers. Nat Chem Biol. 2009; 5:131–134.
27. Kaczor AA, Selent J. Oligomerization of G protein-coupled receptors: biochemical and biophysical methods. Curr Med Chem. 2011; 18:4606–4634.
28. Kerppola TK. Design and implementation of bimolecular fluorescence complementation (BiFC) assays for the visualization of protein interactions in living cells. Nat Protoc. 2006; 1:1278–1286.

29. Trifilieff P, Rives ML, Urizar E, Piskorowski RA, Vishwasrao HD, Castrillon J, Schmauss C, Slattman M, Gullberg M, Javitch JA. Detection of antigen interactions *ex vivo* by proximity ligation assay: endogenous dopamine D_2-adenosine A_{2A} receptor complexes in the striatum. Biotechniques. 2011; 51:111–118.

30. Bellot M, Galandrin S, Boularan C, Matthies HJ, Despas F, Denis C, Javitch J, Mazeres S, Sanni SJ, Pons V, Seguelas MH, Hansen JL, Pathak A, et al. Dual agonist occupancy of AT1-R-alpha2C-AR heterodimers results in atypical G_s-PKA signaling. Nat Chem Biol. 2015; 11:271–279.

31. Chandrasekera PC, Wan TC, Gizewski ET, Auchampach JA, Lasley RD. Adenosine A_1 receptors heterodimerize with $beta_1$- and $beta_2$-adrenergic receptors creating novel receptor complexes with altered G protein coupling and signaling. Cell Signal. 2013; 25:736–742.

32. Navarro G, Cordomi A, Zelman-Femiak M, Brugarolas M, Moreno E, Aguinaga D, Perez-Benito L, Cortes A, Casado V, Mallol J, Canela EI, Lluis C, Pardo L, et al. Quaternary structure of a G-protein-coupled receptor heterotetramer in complex with G_i and G_s. BMC Biol. 2016; 14: 26.

33. Hübner H, Schellhorn T, Gienger M, Schaab C, Kaindl J, Leeb L, Clark T, Möller D, Gmeiner P. Structure-guided development of heterodimer-selective GPCR ligands. Nat Commun. 2016; 7: 12298.

34. Beggiato S, Antonelli T, Tomasini MC, Borelli AC, Agnati LF, Tanganelli S, Fuxe K, Ferraro L. Adenosine A_{2A}-D_2 receptor-receptor interactions in putative heteromers in the regulation of the striato-pallidal gaba pathway: possible relevance for parkinson's disease and its treatment. Curr Protein Pept Sci. 2014; 15:673–680.

35. Guo H, An S, Ward R, Yang Y, Liu Y, Guo XX, Hao Q, Xu TR. Methods used to study the oligomeric structure of G-protein-coupled receptors. Biosci Rep. 2017; 37.

36. Canals M, Marcellino D, Fanelli F, Ciruela F, de Benedetti P, Goldberg SR, Neve K, Fuxe K, Agnati LF, Woods AS, Ferre S, Lluis C, Bouvier M, et al. Adenosine A_{2A}-dopamine D_2 receptor-receptor heteromerization: qualitative and quantitative assessment by fluorescence and bioluminescence energy transfer. J Biol Chem. 2003; 278:46741–46749.

37. Canals M, Burgueno J, Marcellino D, Cabello N, Canela EI, Mallol J, Agnati L, Ferre S, Bouvier M, Fuxe K, Ciruela F, Lluis C, Franco R. Homodimerization of adenosine A_{2A} receptors: qualitative and quantitative assessment by fluorescence and bioluminescence energy transfer. J Neurochem. 2004; 88:726–734.

38. Greenwood C, Ruff D, Kirvell S, Johnson G, Dhillon HS, Bustin SA. Proximity assays for sensitive quantification of proteins. Biomol Detect Quantif. 2015; 4:10–16.

39. Müller CE, Maurinsh J, Sauer R. Binding of [^{3}H]MSX-2 (3-(3-hydroxypropyl)-7-methyl-8-(*m*-methoxystyryl)-1-propargylxanthine) to rat striatal membranes-a new, selective antagonist radioligand for A_{2A} adenosine receptors. Eur J Pharm Sci. 2000; 10:259–265.

40. Bonaventura J, Navarro G, Casado-Anguera V, Azdad K, Rea W, Moreno E, Brugarolas M, Mallol J, Canela EI, Lluis C, Cortes A, Volkow ND, Schiffmann SN, et al. Allosteric interactions between agonists and antagonists within the adenosine A_{2A} receptor-dopamine D_2 receptor heterotetramer. Proc Natl Acad Sci U S A. 2015; 112: E3609–3618.

41. May LT, Bridge LJ, Stoddart LA, Briddon SJ, Hill SJ. Allosteric interactions across native adenosine-A_3 receptor homodimers: quantification using single-cell ligand-binding kinetics. FASEB J. 2011; 25:3465–3476.

42. Moriyama K, Sitkovsky MV. Adenosine A_{2A} receptor is involved in cell surface expression of A_{2B} receptor. J Biol Chem. 2010; 285:39271–39288.

43. Fernandez-Gallardo M, Gonzalez-Ramirez R, Sandoval A, Felix R, Monjaraz E. Adenosine Stimulate Proliferation and Migration in Triple Negative Breast Cancer Cells. PLoS One. 2016; 11:e0167445.

44. Panjehpour M, Castro M, Klotz KN. Human breast cancer cell line MDA-MB-231 expresses endogenous A_{2B} adenosine receptors mediating a Ca^{2+} signal. Br J Pharmacol. 2005; 145:211–218.

45. Phelps PT, Anthes JC, Correll CC. Characterization of adenosine receptors in the human bladder carcinoma T24 cell line. Eur J Pharmacol. 2006; 536:28–37.

46. Borroto-Escuela DO, Romero-Fernandez W, Tarakanov AO, Gomez-Soler M, Corrales F, Marcellino D, Narvaez M, Frankowska M, Flajolet M, Heintz N, Agnati LF, Ciruela F, Fuxe K. Characterization of the A_{2A}R-D_2R interface: focus on the role of the C-terminal tail and the transmembrane helices. Biochem Biophys Res Commun. 2010; 402:801–807.

47. Van der Ploeg I, Ahlberg S, Parkinson FE, Olsson RA, Fredholm BB. Functional characterization of adenosine A_2 receptors in Jurkat cells and PC12 cells using adenosine receptor agonists. Naunyn Schmiedebergs Arch Pharmacol. 1996; 353:250–260.

48. Mirabet M, Mallol J, Lluis C, Franco R. Calcium mobilization in Jurkat cells via A_{2B} adenosine receptors. Br J Pharmacol. 1997; 122:1075–1082.

49. Feoktistov I, Biaggioni I. Pharmacological characterization of adenosine A_{2B} receptors: studies in human mast cells co-expressing A_{2A} and A_{2B} adenosine receptor subtypes. Biochem Pharmacol. 1998; 55:627–633.

50. Hide I, Padgett WL, Jacobson KA, Daly JW. A_{2A} adenosine receptors from rat striatum and rat pheochromocytoma PC12 cells: characterization with radioligand binding and by activation of adenylate cyclase. Mol Pharmacol. 1992; 41:352–359.

51. Sanjani MS, Teng B, Krahn T, Tilley S, Ledent C, Mustafa SJ. Contributions of A_{2A} and A_{2B} adenosine receptors in coronary flow responses in relation to the KATP channel

using A_{2B} and $A_{2A}/_{2B}$ double-knockout mice. Am J Physiol Heart Circ Physiol. 2011; 301:H2322–2333.

52. Bruzzese L, Fromonot J, By Y, Durand-Gorde JM, Condo J, Kipson N, Guieu R, Fenouillet E, Ruf J. NF-kappaB enhances hypoxia-driven T-cell immunosuppression via upregulation of adenosine A_{2A} receptors. Cell Signal. 2014; 26:1060–1067.

53. Rozenfeld R, Gupta A, Gagnidze K, Lim MP, Gomes I, Lee-Ramos D, Nieto N, Devi LA. AT_1R-$CB(_1)$ R heteromerization reveals a new mechanism for the pathogenic properties of angiotensin II. EMBO J. 2011; 30:2350–2363.

54. Elder AD, Domin A, Kaminski Schierle GS, Lindon C, Pines J, Esposito A, Kaminski CF. A quantitative protocol for dynamic measurements of protein interactions by Förster resonance energy transfer-sensitized fluorescence emission. J R Soc Interface. 2009; 6:59–81.

55. Shyu YJ, Suarez CD, Hu CD. Visualization of ternary complexes in living cells by using a BiFC-based FRET assay. Nature Protocols. 2008; 3:1693–1702.

56. Borroto-Escuela DO, Romero-Fernandez W, Garriga P, Ciruela F, Narvaez M, Tarakanov AO, Palkovits M, Agnati LF, Fuxe K. G protein-coupled receptor heterodimerization in the brain. Methods Enzymol. 2013; 521:281–294.

57. Schiedel AC, Hinz S, Thimm D, Sherbiny F, Borrmann T, Maass A, Müller CE. The four cysteine residues in the second extracellular loop of the human adenosine A_{2B} receptor: role in ligand binding and receptor function. Biochem Pharmacol. 2011; 82:389–399.

58. Lowry OH, Rosebrough NJ, Farr AL, Randall RJ. Protein measurement with the Folin phenol reagent. J Biol Chem. 1951; 193:265–275.

59. Borrmann T, Hinz S, Bertarelli DC, Li W, Florin NC, Scheiff AB, Müller CE. 1-alkyl-8-(piperazine-1-sulfonyl) phenylxanthines: development and characterization of adenosine A_{2B} receptor antagonists and a new radioligand with subnanomolar affinity and subtype specificity. J Med Chem. 2009; 52:3994–4006.

60. Hinz S, Lacher SK, Seibt BF, Müller CE. BAY60-6583 acts as a partial agonist at adenosine A_{2B} receptors. J Pharmacol Exp Ther. 2014; 349:427–436.

61. Nordstedt C, Fredholm BB. A modification of a protein-binding method for rapid quantification of cAMP in cell-culture supernatants and body fluid. Anal Biochem. 1990; 189:231–234.

62. Navarro G, Quiroz C, Moreno-Delgado D, Sierakowiak A, McDowell K, Moreno E, Rea W, Cai NS, Aguinaga D, Howell LA, Hausch F, Cortes A, Mallol J, et al. Orexin-corticotropin-releasing factor receptor heteromers in the ventral tegmental area as targets for cocaine. J Neurosci. 2015; 35:6639–6653.